ES2013: The 25th Annual Workshop on Recent Developments in Electronic Structure Methods
June 11-14 2013
CWM, Williamsburg, VA

Dynamical screening effects from first principles:

Implication for low-energy models and application to the iron pnictides

M. Casula*, P. Werner, F. Aryasetiawan, T. Miyake, L. Vaugier, A. Rubtsov, A. J. Millis, and S. Biermann

* CNRS & Institut de Minéralogie et de Physique des Milieux Condensés, Université Pierre et Marie Curie, Paris

Iron-pnictides: high-T_c superconductors

- Discovery of high-T_c in pnictides in 2008: new excitement
- Electron-phonon coupling cannot account for T_c
- New family of unconventional high-T_c superconductors: cuprates are not the only ones!
- Proximity of spin ordered phases
- Multi-band physics

$BaFe_2As_2$

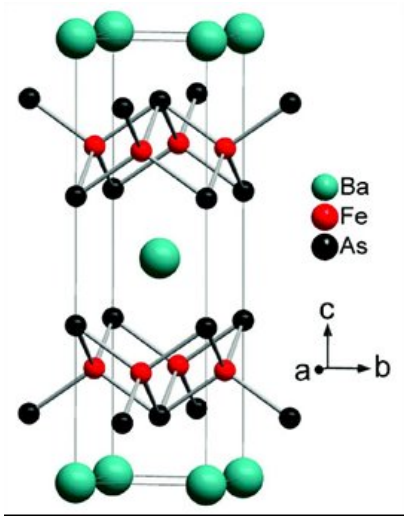

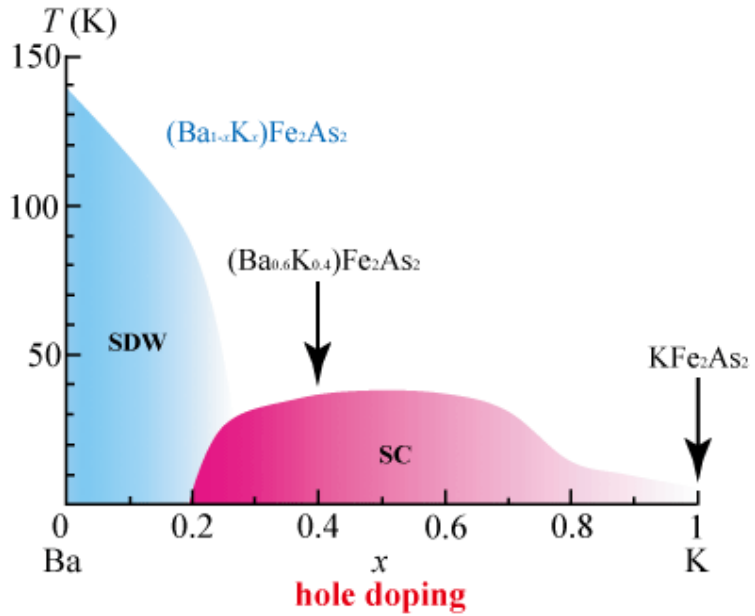

Correlation level?

Pairing symmetry and superconducting mechanism?

Can first principle calculations account for the spectral properties and the phase diagram?

Angle resolved photoemission spectroscopy (ARPES) in $BaFe_2As_2$

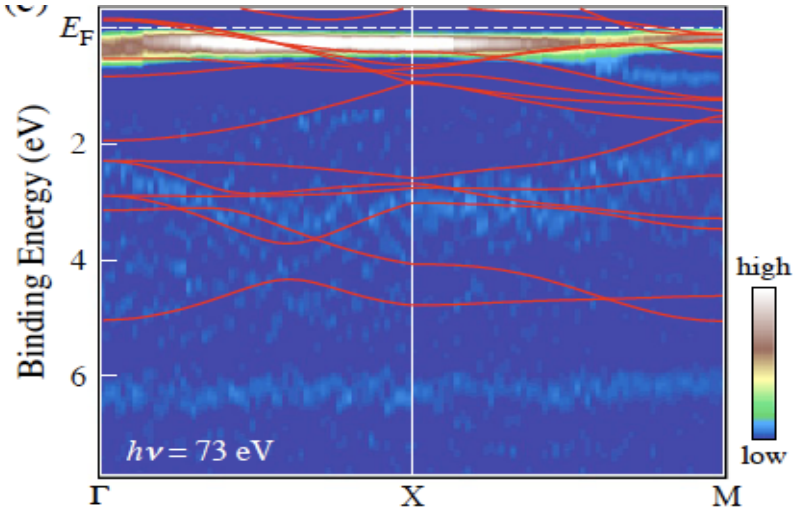

Ding et al., J. Phys.: Cond. Matter **23**, 135701 (2011)

de Jong et al. Phys. Rev. B **79**, 115125 (2009)

and many others….

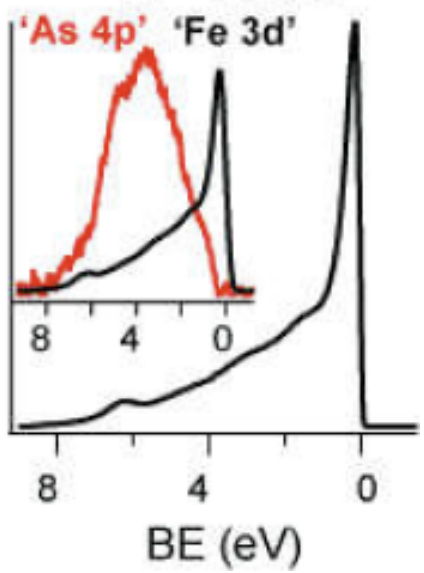

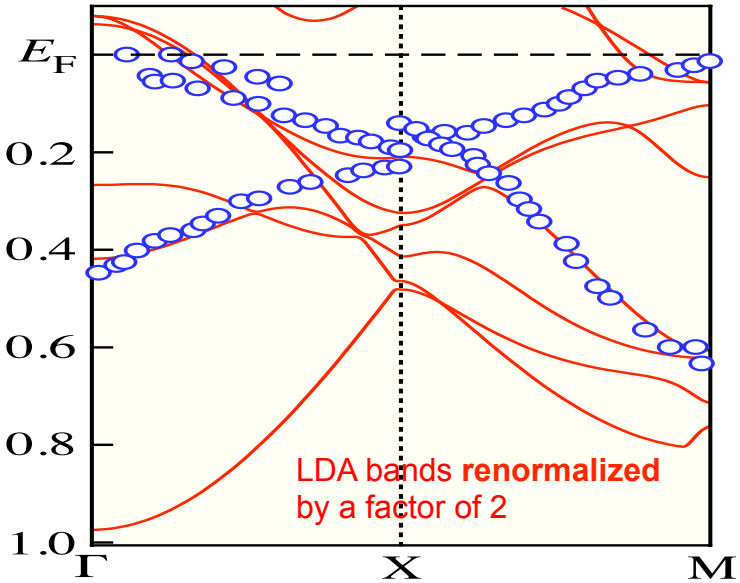

DFT-LDA band structure resembles ARPES only after **band renormalization** (usually a factor in the range of 2-5)

ARPES satellites are missing

Need of improved theories for an *ab-initio* description of correlated materials

Outline

- Constructing effective models for correlated materials: dynamical (frequency dependent) onsite interaction U from reducing the Hamiltonian to correlated bands
- Satellites and low-energy properties of $BaFe_2As_2$ from dynamical mean field theory (DMFT) with frequency dependent U
- Low-energy Hamiltonian for frequency dependent U

Low-energy model of correlated materials

Tight-binding model from localized (Wannier) orbitals

$$H = \sum_{\{im\sigma\}} (H^{\mathrm{LDA}}_{im,i'm'} - H^{\text{double counting}}_{im,i'm'}) a^{\dagger}_{im\sigma} a_{i'm'\sigma}$$

$$+ \frac{1}{2} \sum_{\substack{imm'\sigma \\ \text{(correl. orb.)}}} V_{mm'} n_{im\sigma} n_{im'-\sigma} + \frac{1}{2} \sum_{\substack{im\neq m'\sigma \\ \text{(correl. orb.)}}} (V_{mm'} - J_{mm'}) n_{im\sigma} n_{im'\sigma}$$

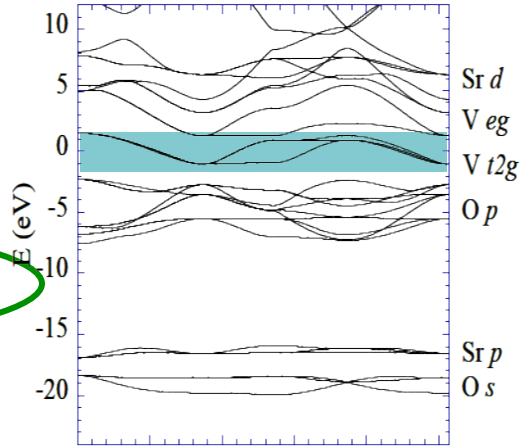

Density-density interactions
(matrix elements of the Coulomb potential in the Wannier basis)

Those interactions are screened

by the excluded (high-energy) degrees of freedom

cRPA screened interaction

- *Screening coming from the electrons excluded from the model*
- RPA screening:

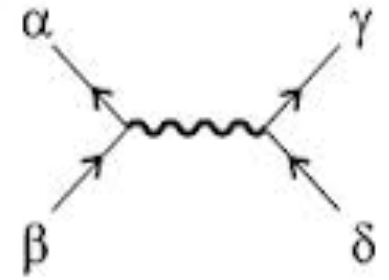

$$U(\omega) = \frac{\upsilon}{1 - P_r(\omega)\upsilon}$$

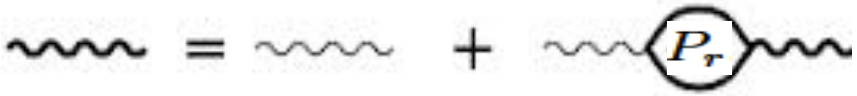

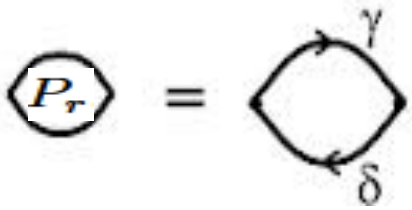

RPA polarization: e-h pair excitations

$$P(\mathbf{r},\mathbf{r}';\omega) = \sum_{i}^{occ}\sum_{j}^{unocc} \psi_i(\mathbf{r})\psi_i^*(\mathbf{r}')\psi_j^*(\mathbf{r})\psi_j(\mathbf{r}') \times \left\{ \frac{1}{\omega - \varepsilon_j + \varepsilon_i + i0^+} - \frac{1}{\omega + \varepsilon_j - \varepsilon_i - i0^+} \right\}$$

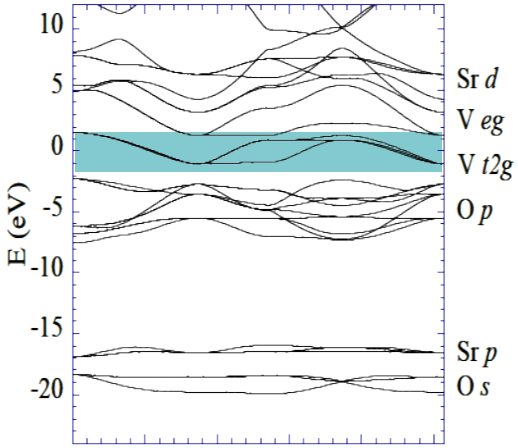

Total polarizability $P = P_d + P_r$

P_d d-d transitions

P_r other transitions

Aryasetiawan et al. PRB **70**, 195104 (2004)
Miyake et al. **80**, 155134 (2009)
Miyake et al. **61**, 7172 (2000)

Dynamic U in $BaFe_2As_2$

- **Downfolding** the full LDA Hamiltonian by Fe-3d and As-4p max localized Wannier functions

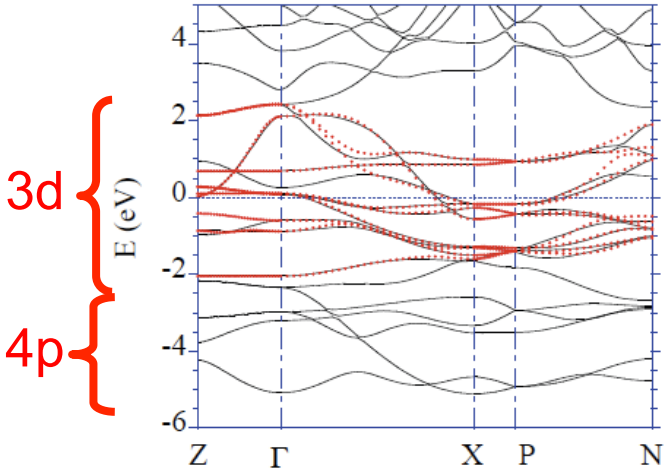

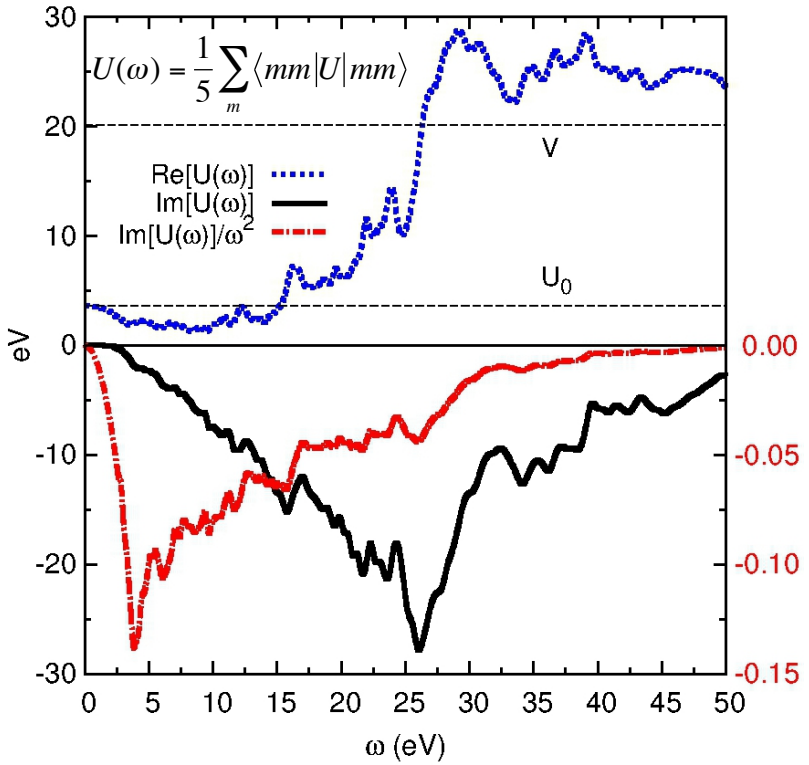

- Coulomb interaction:
  frequency dependence from cRPA,
  Slater parameterization for static part of U

- Important observations:

1. **Static value very different from the unscreened** (infinite frequency) limit
2. **Strong frequency dependence** even at low energy scale

Dynamic U and mapping to bosons

- **Downfolding** the full LDA Hamiltonian by Fe-3d and As-4p max localized Wannier functions

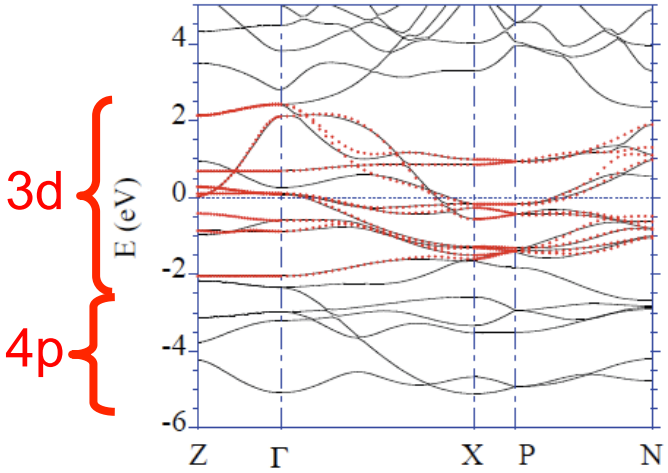

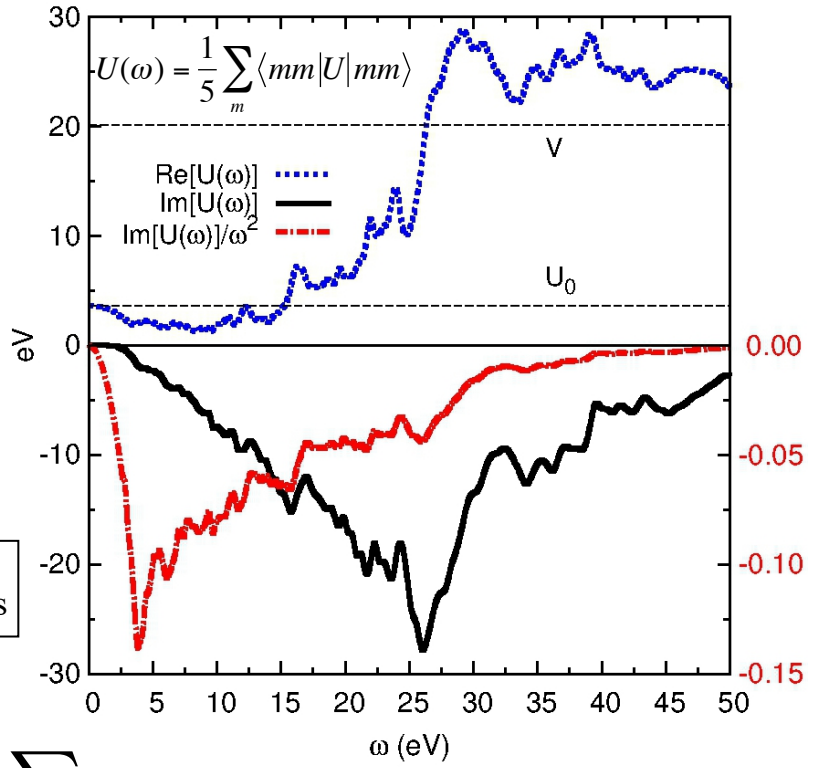

$$H = H_{\text{multi-band Hubbard with STATIC U}} + H_{\text{plasmons}}$$

$$H_{\text{plasmons}} = \sum_{i,\nu} \omega_\nu b^\dagger_{i\nu} b_{i\nu} + \sum_{i,\nu} \lambda_\nu (b^\dagger_{i\nu} + b_{i\nu}) \sum_{m,\sigma} n_{im\sigma}$$

$$\lambda_\nu^2 = -\frac{1}{\pi}\text{Im}[U(\omega_\nu)]$$ Electron-plasmon coupling given by ImU

Hubbard-Holstein model: plasmons interacting with correlated electrons

$$H = \sum_{\vec{k}\sigma} \epsilon(\vec{k}) c^{\dagger}_{\vec{k}\sigma} c_{\vec{k}\sigma} + U \sum_i n_{i\uparrow} n_{i\downarrow} + \omega_0 \sum_i b^{\dagger}_i b_i$$

$$+ g \sum_i (b^{\dagger}_i + b_i)(n_{i\uparrow} + n_{i\downarrow} - 1).$$

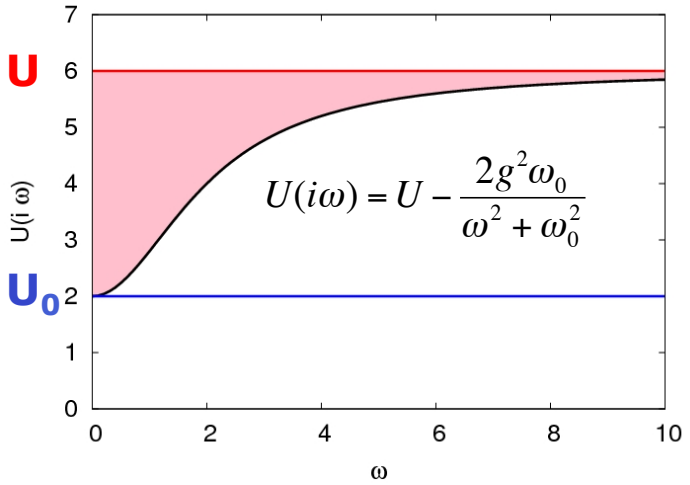

Spectral function with β=100, ω_0=10, U=6.5 and g=4.7 on the Bethe lattice

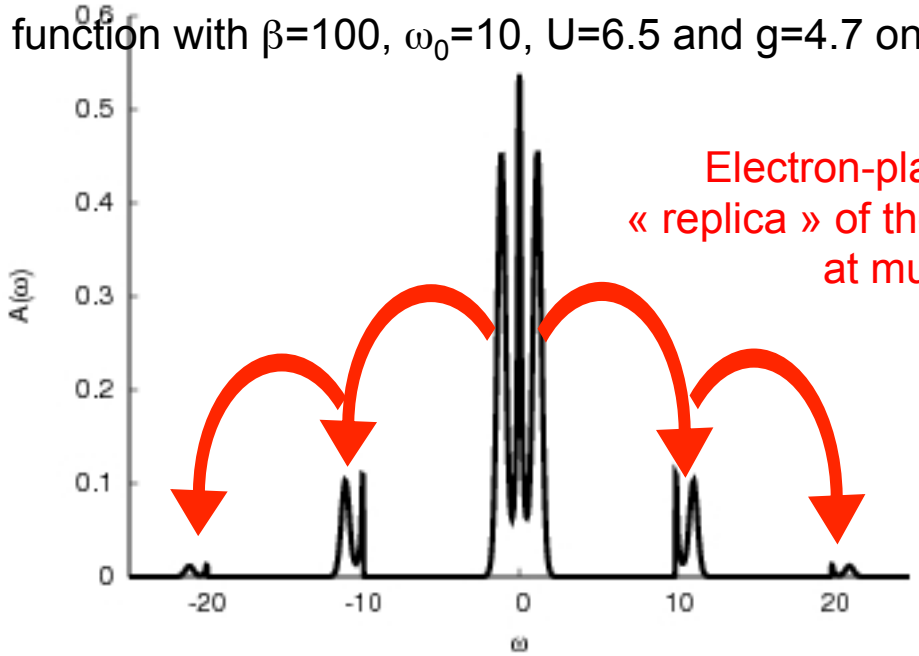

Electron-plasmon excitations:
« replica » of the low-energy structure
at multiples of ω_0

Dynamical mean-field approach

Accurate description of **local atomic physics** is essential in case of strong correlation

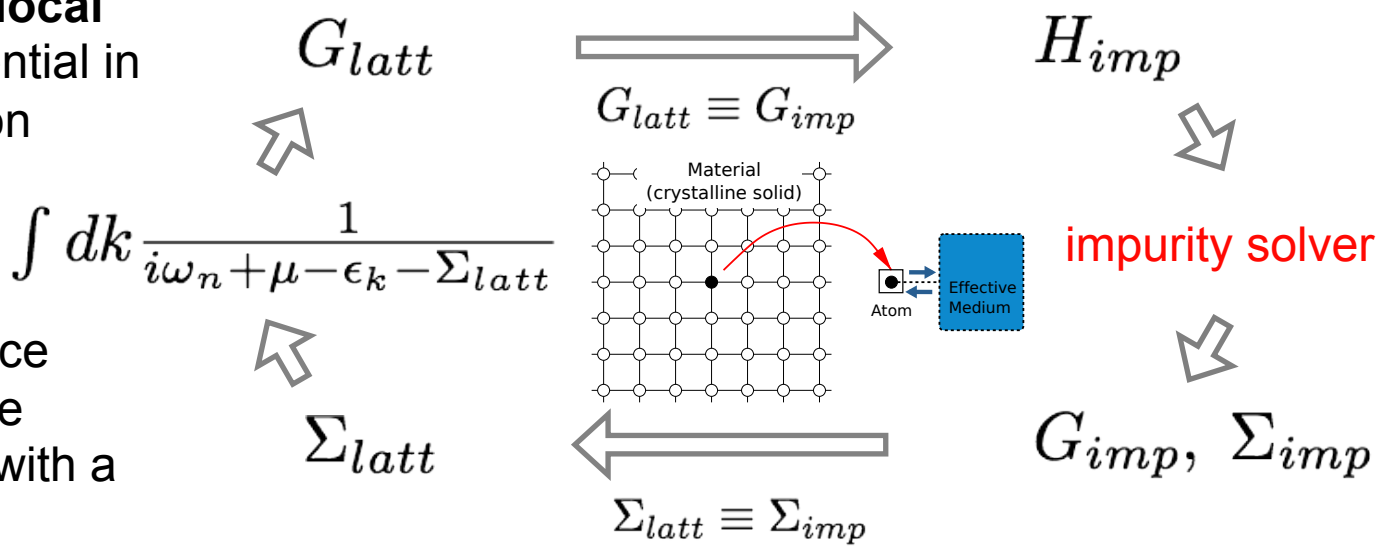

DMFT maps the full lattice problem into a single site Hamiltonian hybridized with a self-consistent bath

A. Georges, G. Kotliar, W. Krauth, M. Rozenberg, RMP **68**, 13 (1996)

Resolution of the impurity problem by the hybridization expansion CTQMC algorithm which supports retarded interactions (Werner and Millis, PRL 2006)

$Ba_{(1-2x)}K_{2x}Fe_2As_2$: x-T phase space

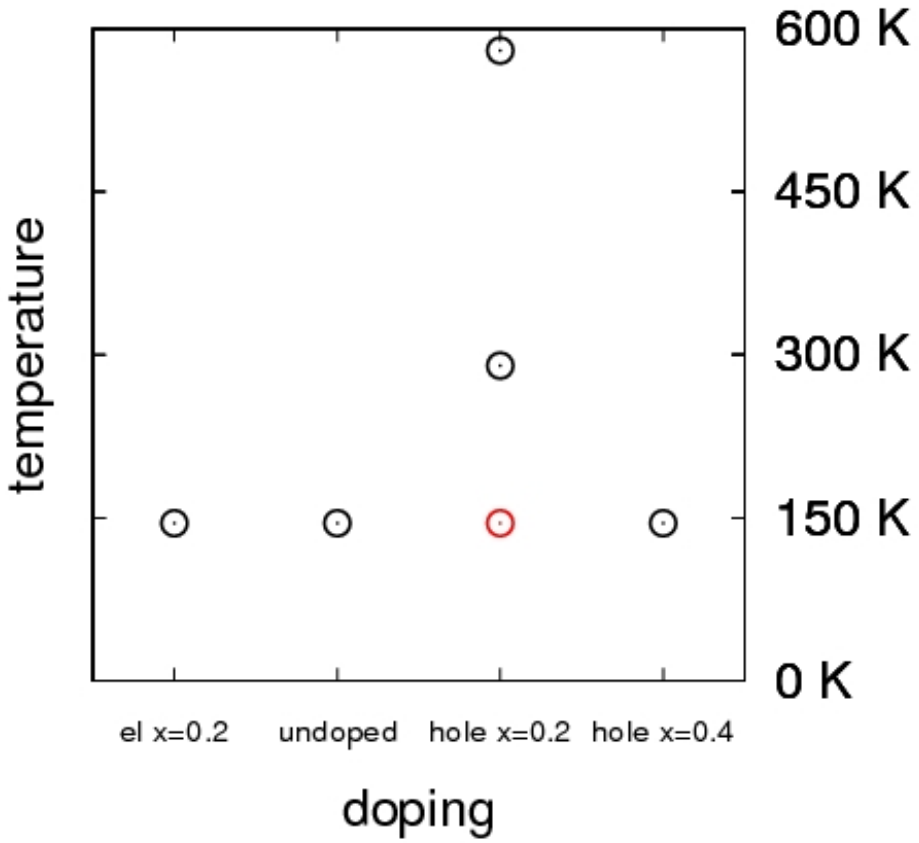

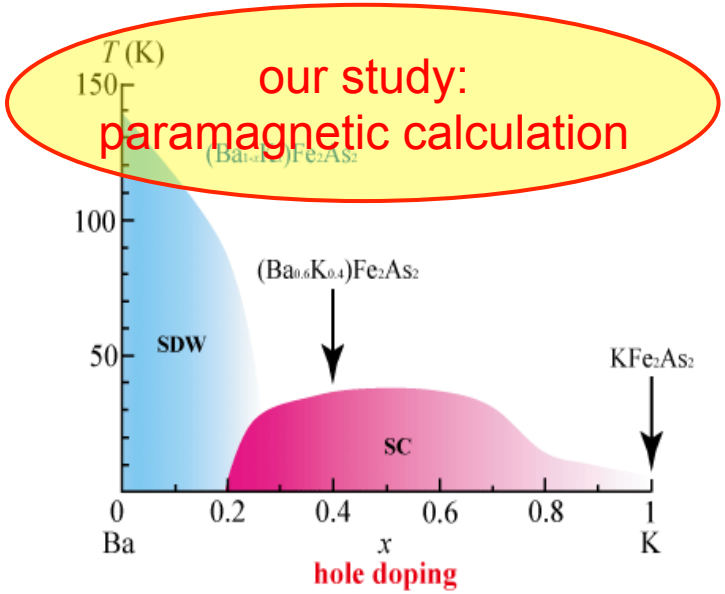

Dynamic U effects in $Ba_{0.6}K_{0.4}Fe_2As_2$

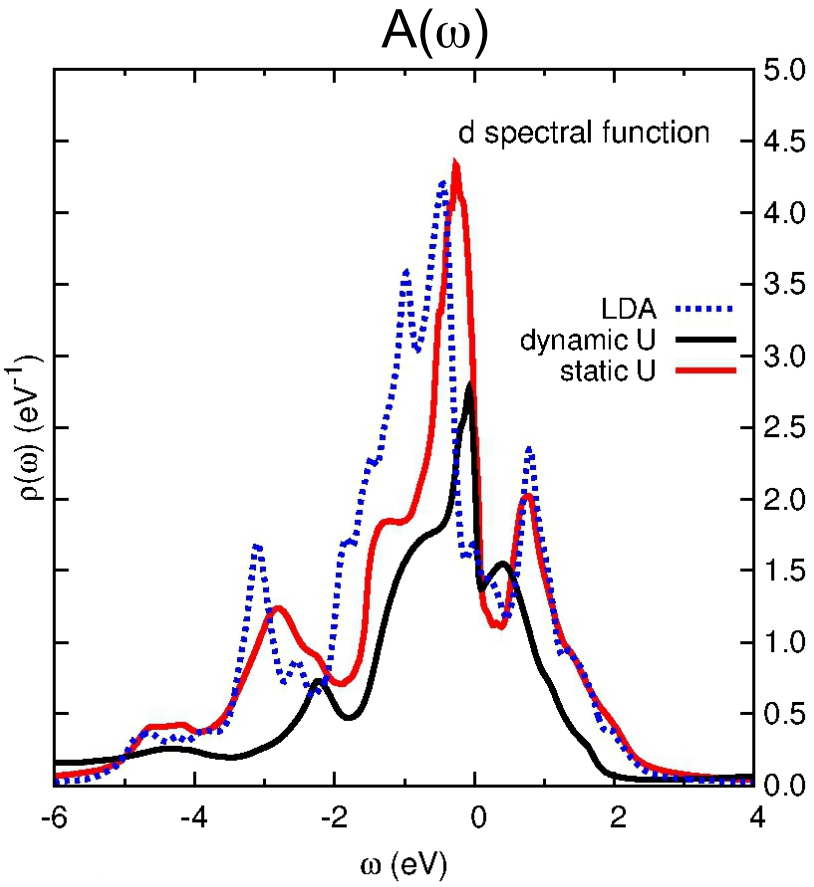

Dynamic U effects in $Ba_{0.6}K_{0.4}Fe_2As_2$

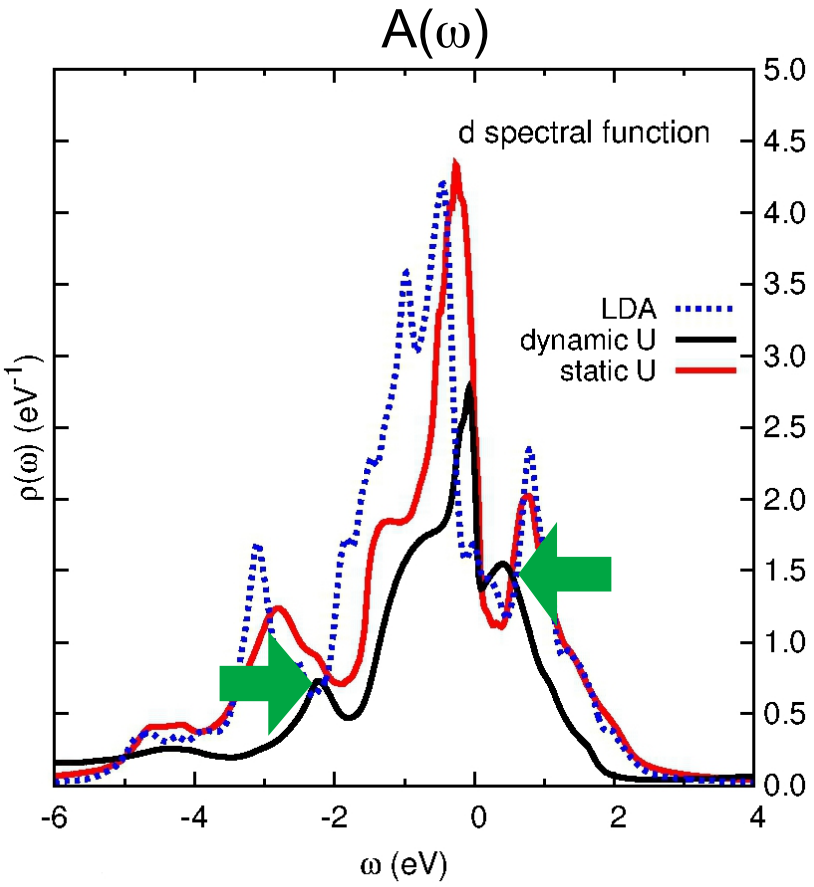

Structures from p-d hybridization squeezed toward the Fermi energy

Dynamic U effects in $Ba_{0.6}K_{0.4}Fe_2As_2$

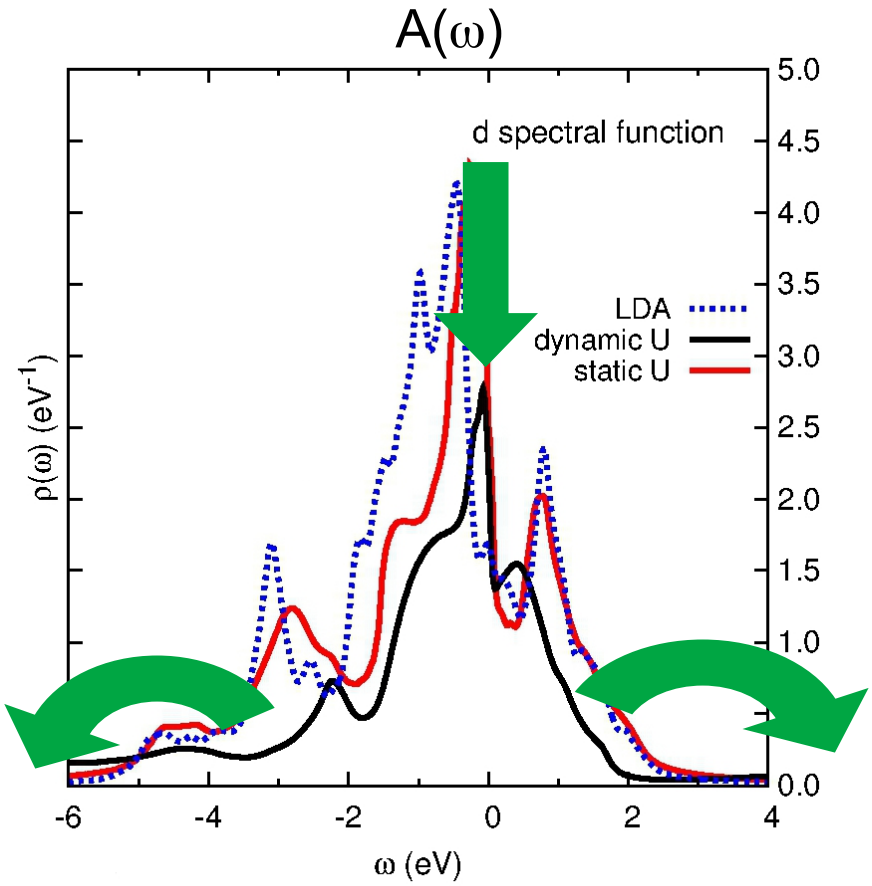

Weight reduction at low-energy and spectral weight transfer to high-energy

Dynamic U effects in $Ba_{0.6}K_{0.4}Fe_2As_2$

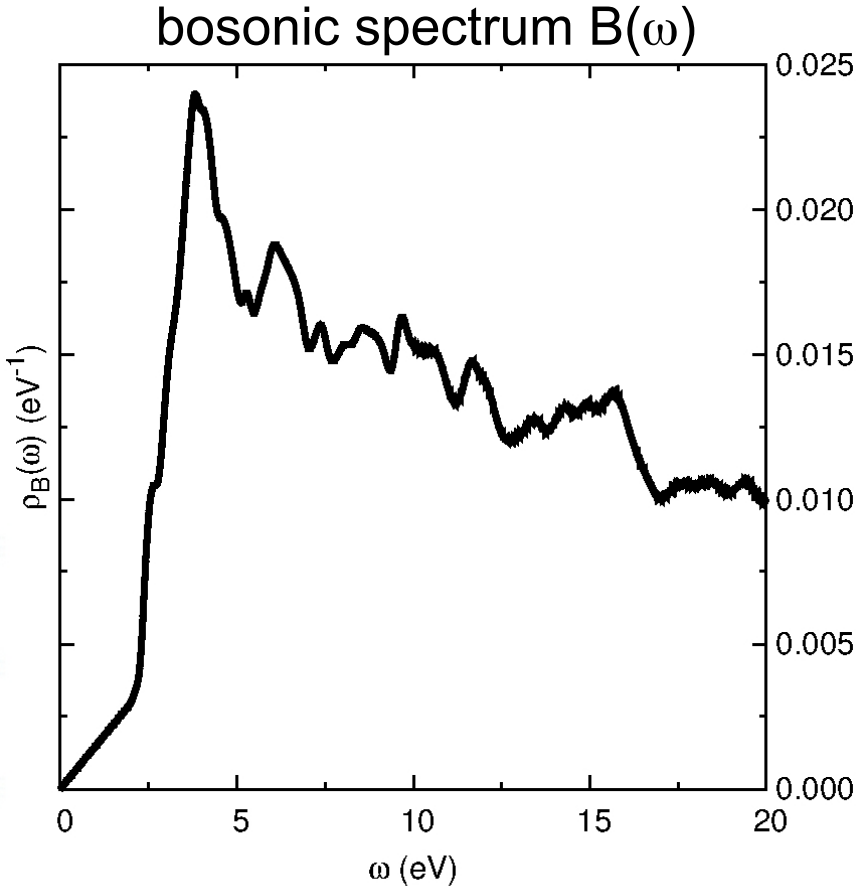

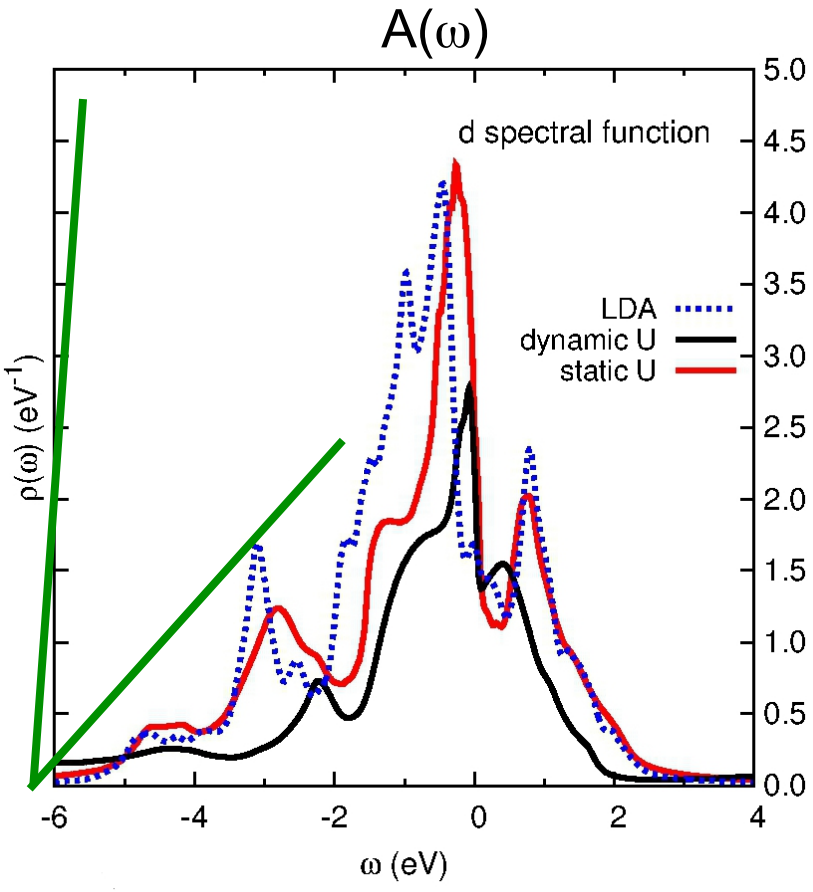

$$A(\omega) = \int d\varepsilon\, B(\varepsilon) \frac{1 + e^{-\beta\omega}}{(1 + e^{-\beta(\varepsilon-\omega)})(1 - e^{-\beta\varepsilon})} A_0(\omega - \varepsilon)$$

Dynamic U effects in $Ba_{0.6}K_{0.4}Fe_2As_2$

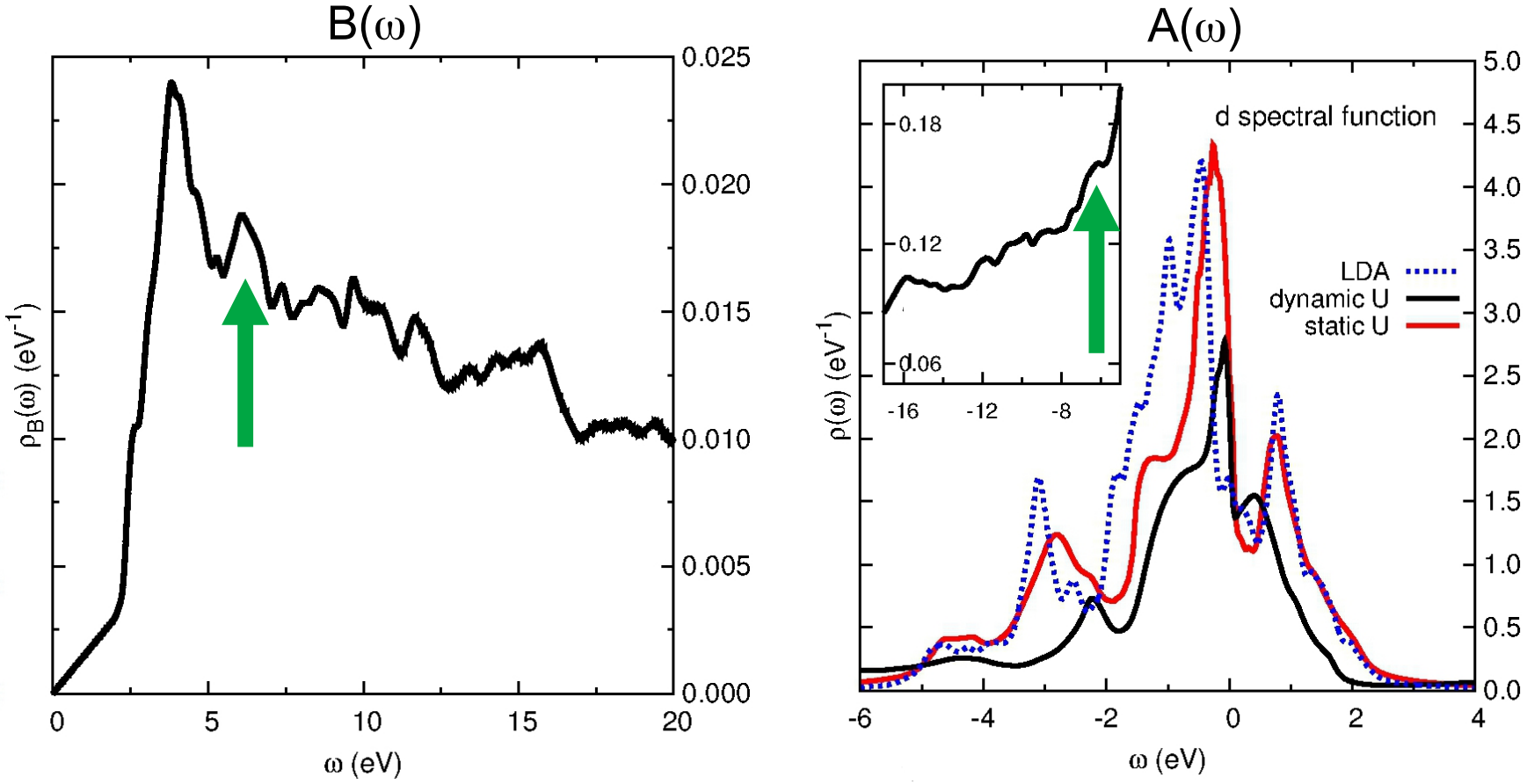

Satellites: at 6.1 eV

Dynamic U effects in $Ba_{0.6}K_{0.4}Fe_2As_2$

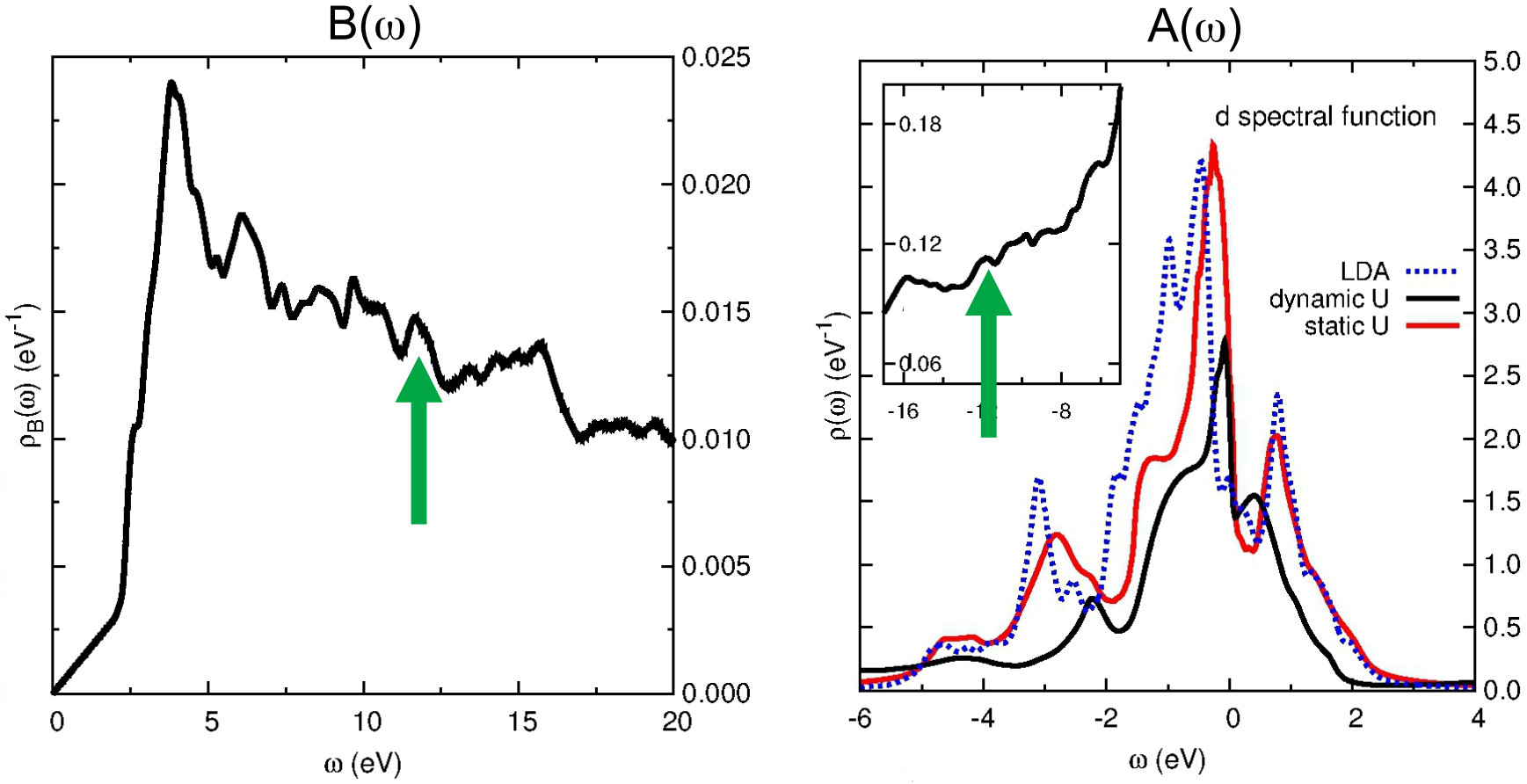

Satellites: at 12 eV

Dynamic U effects in $Ba_{0.6}K_{0.4}Fe_2As_2$

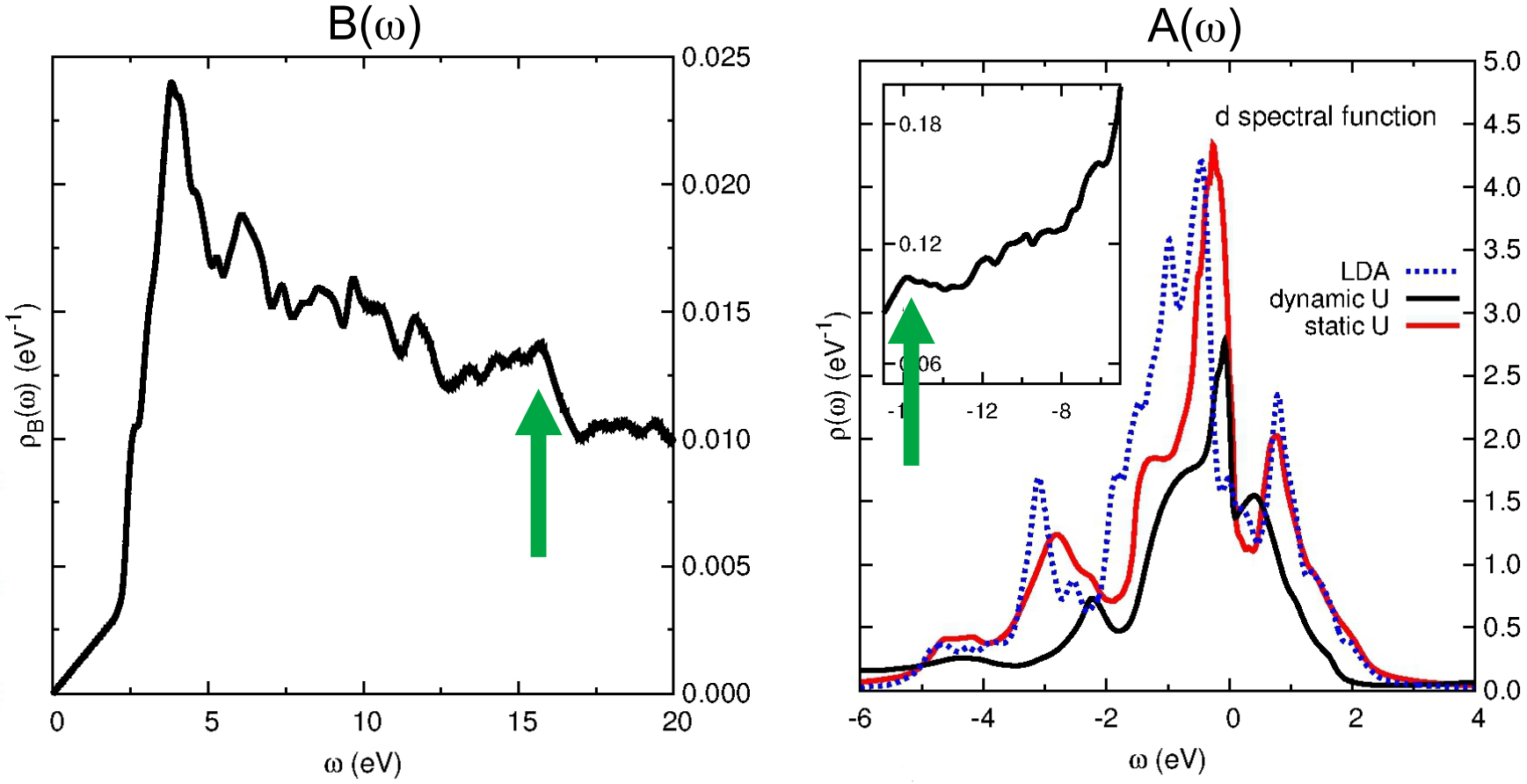

Satellites: at 16 eV

Experimental signatures of d-satellites from ARPES?

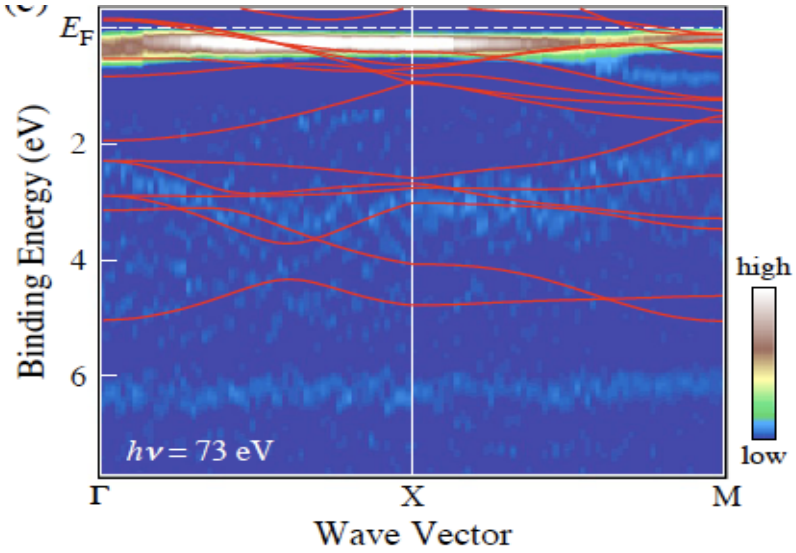

Ding et al., J. Phys.: Cond. Matter **23**, 135701 (2011)

de Jong et al. Phys. Rev. B **79**, 115125 (2009)

Veronique Brouet, private communication

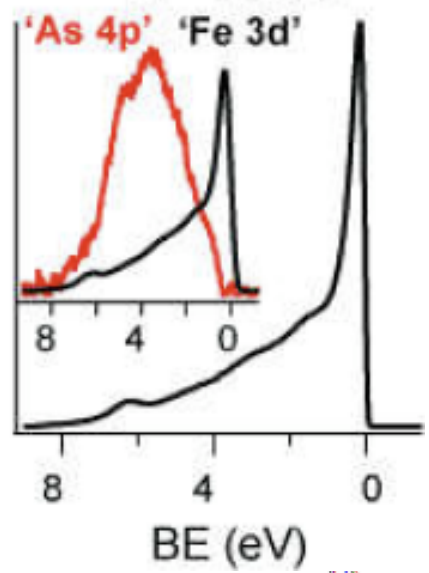

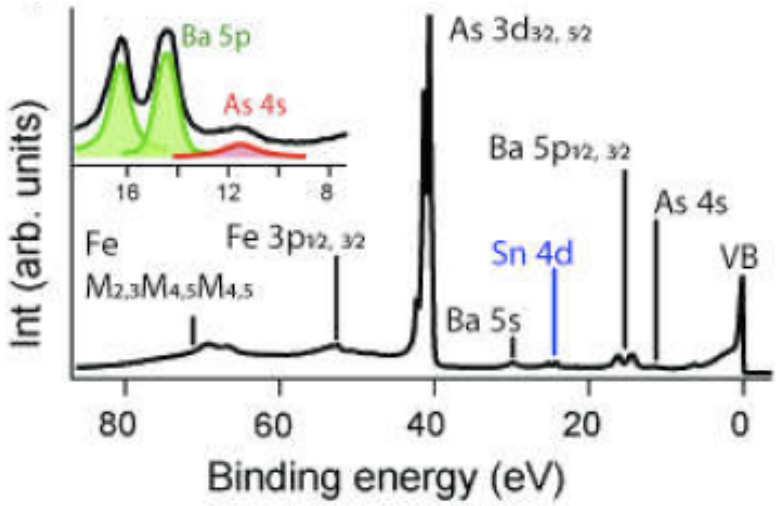

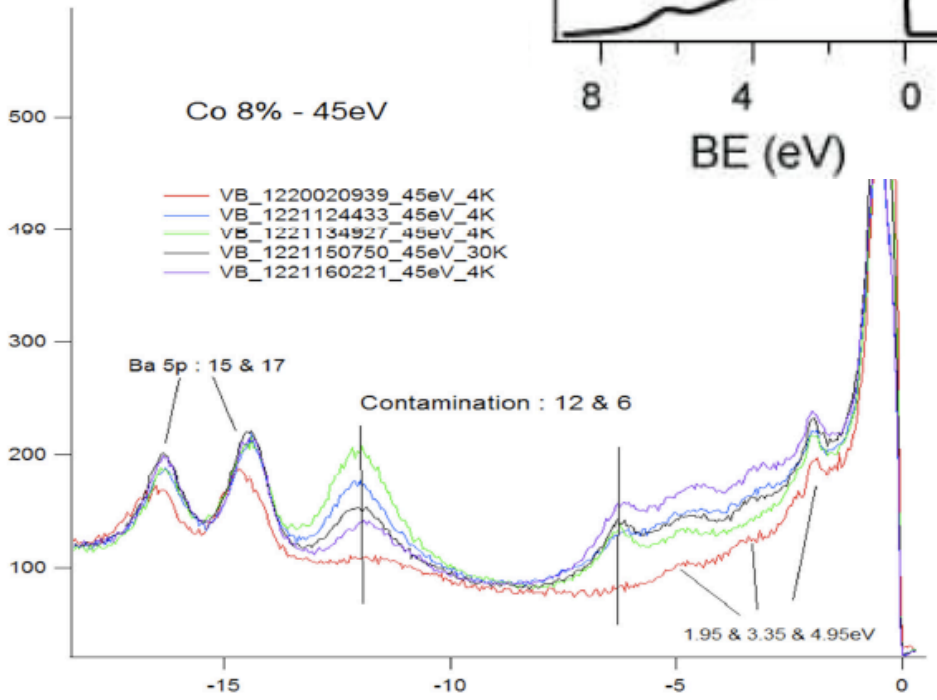

Doping dependence in the self energy

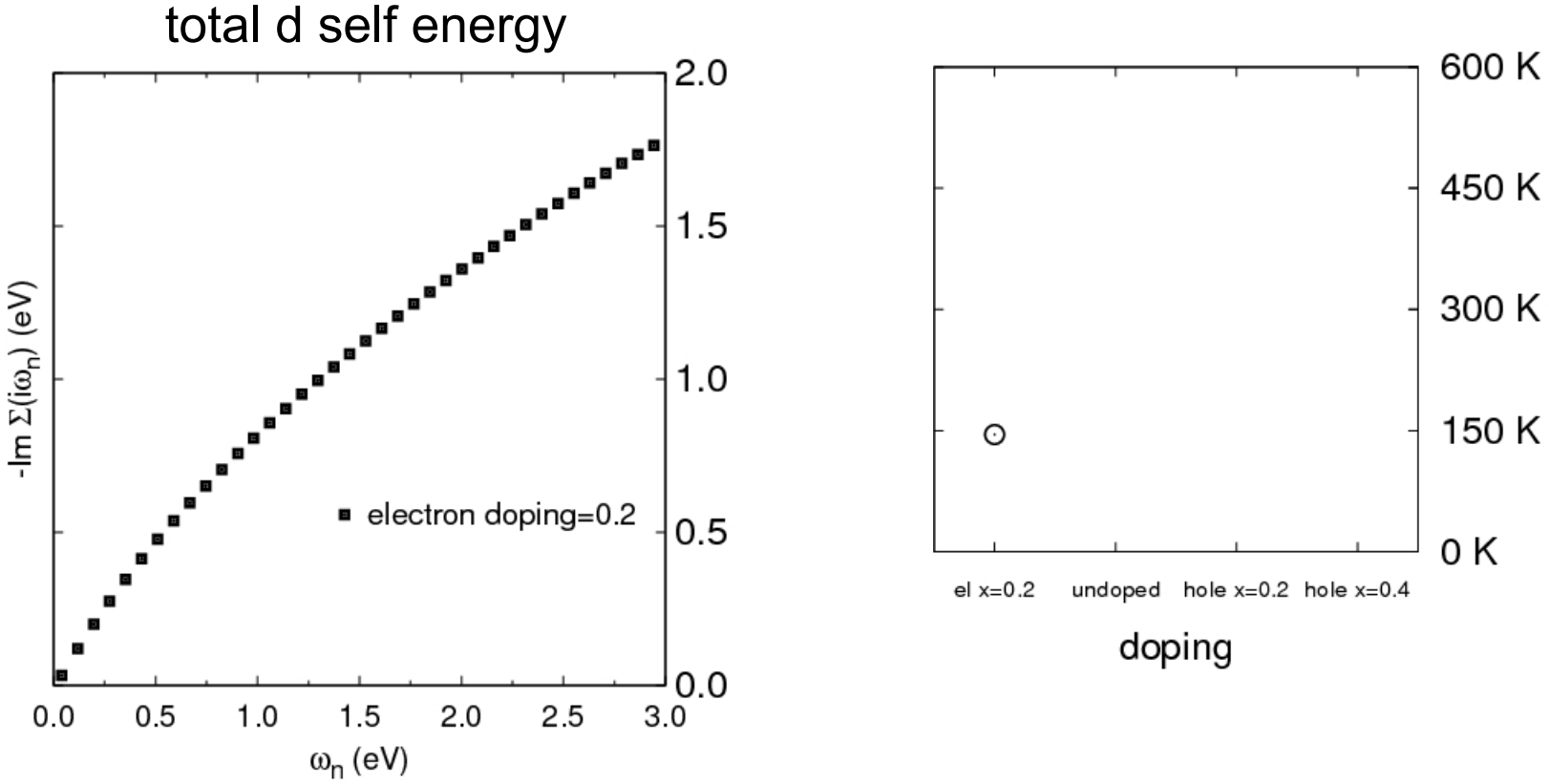

Doping dependence in the self energy

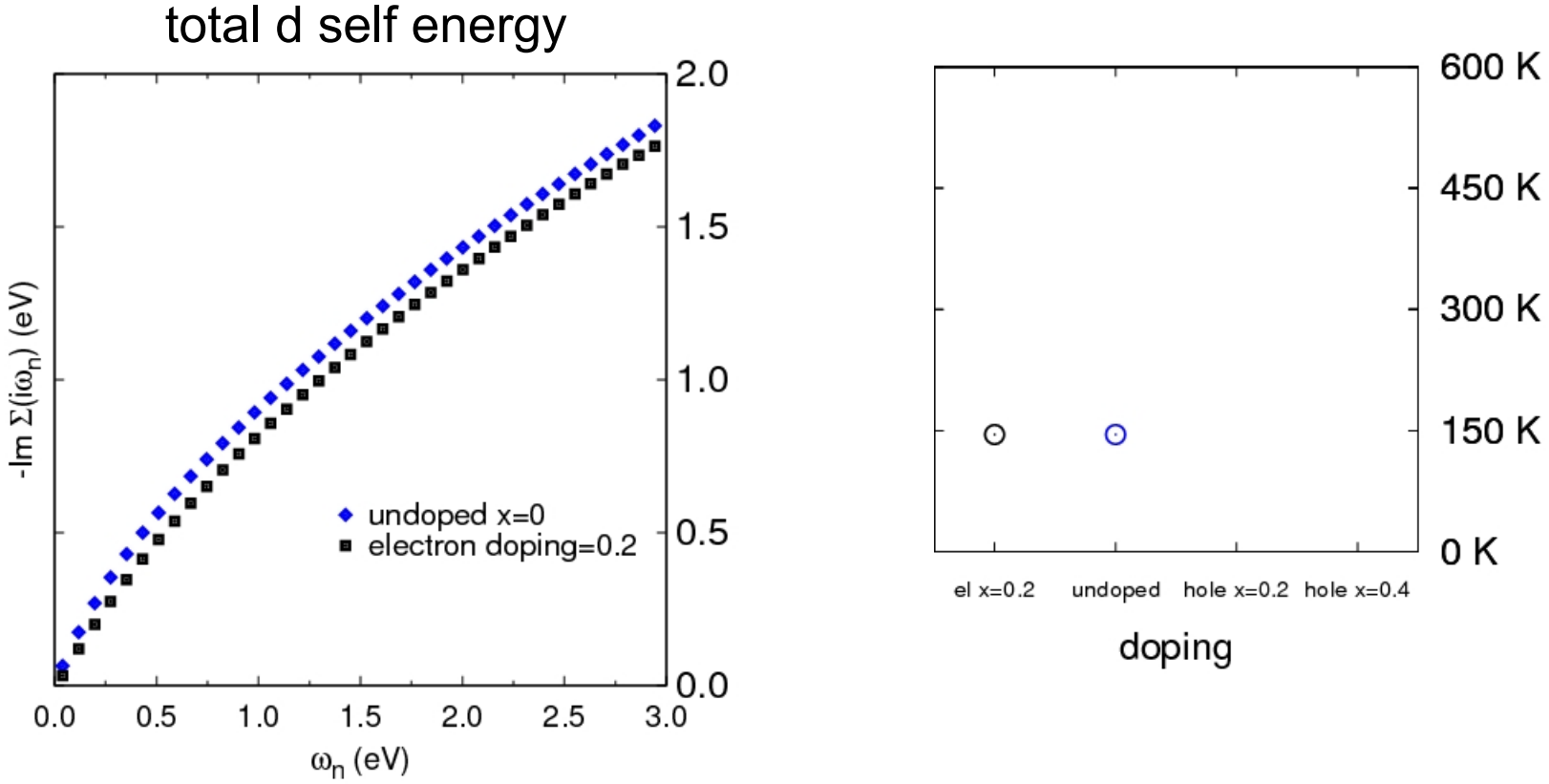

Doping dependence in the self energy

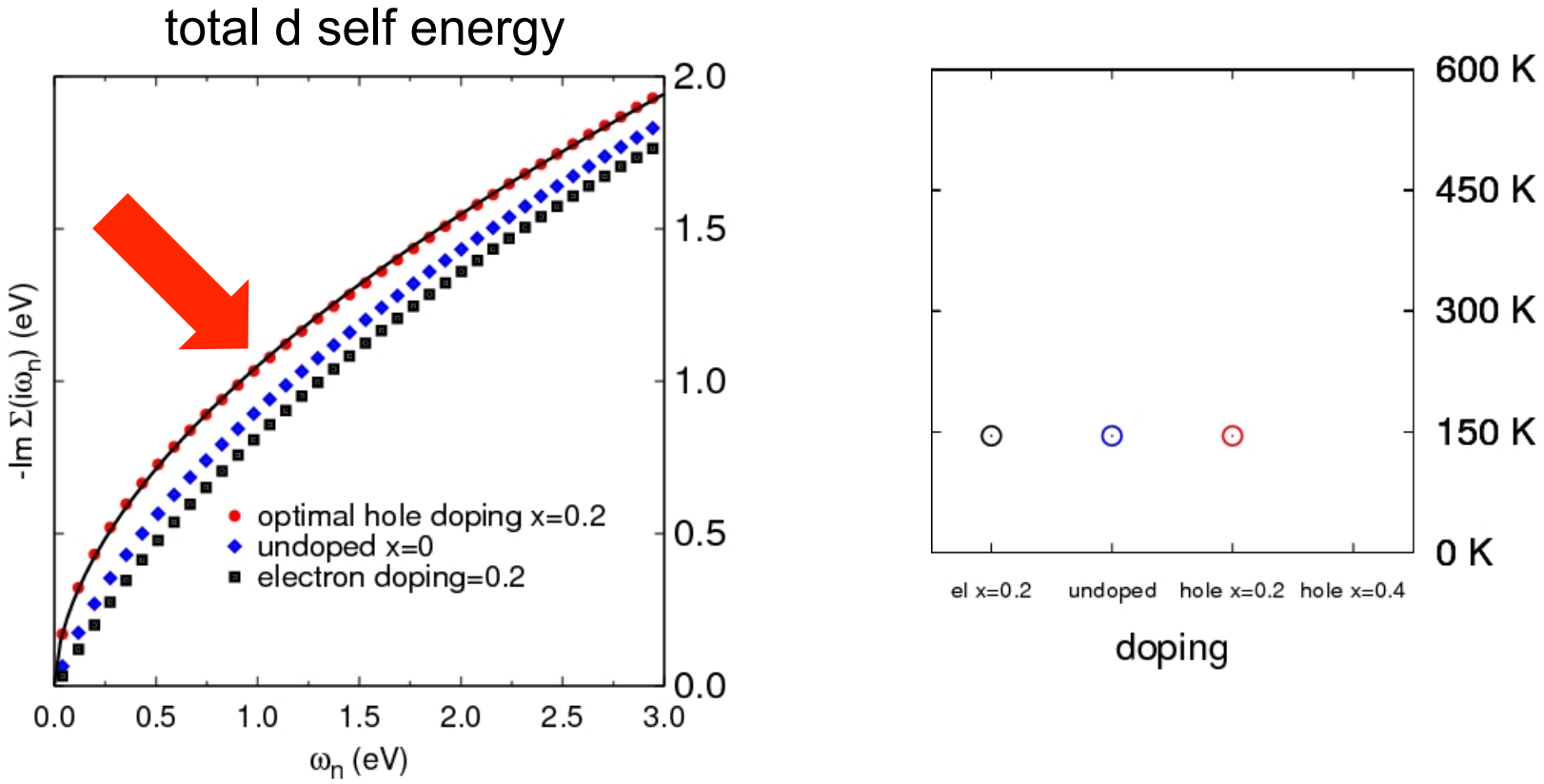

Onset of the square root behavior at optimal hole doping

NON FERMI LIQUID BEHAVIOR

Doping dependence in the self energy

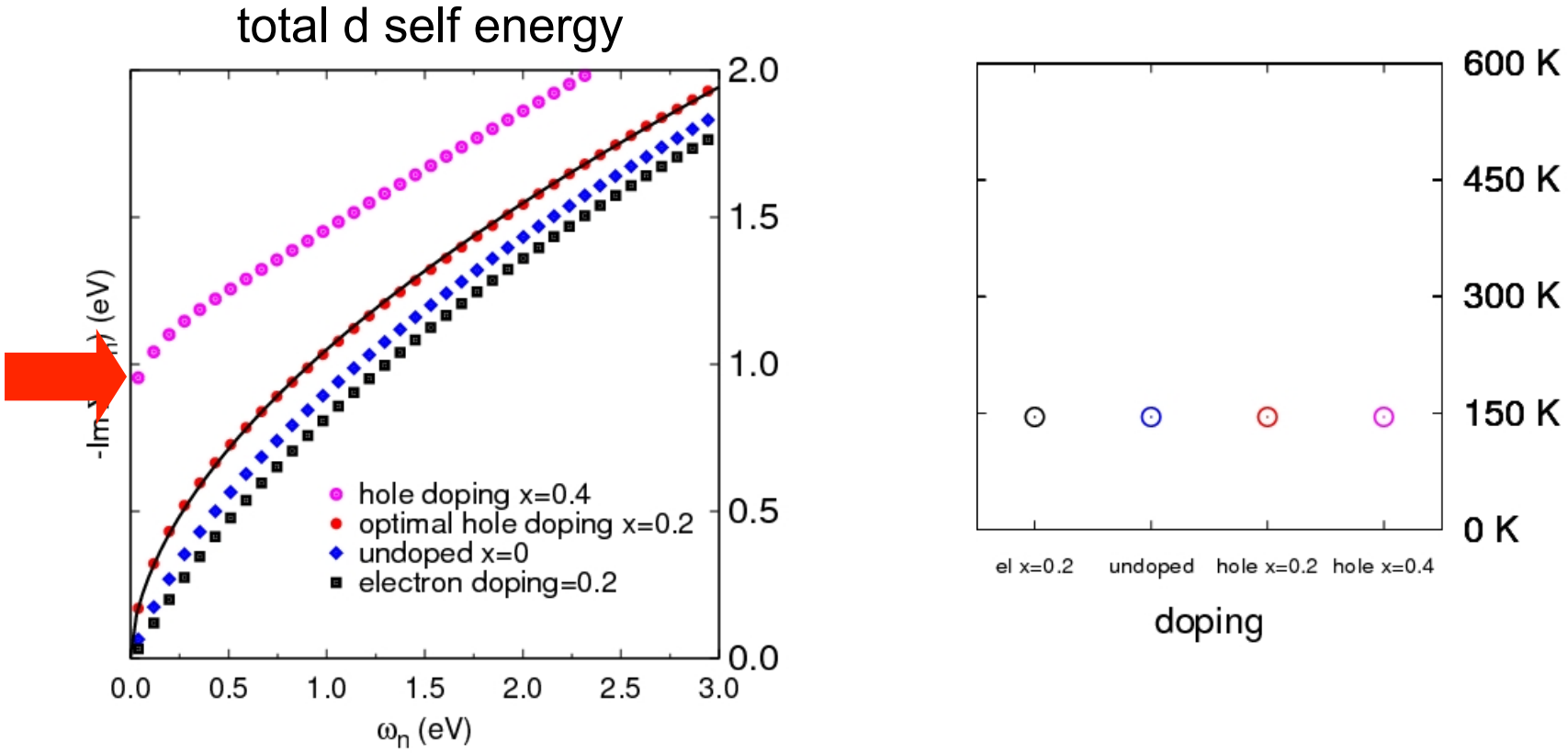

Close to the full substitution (KFe_2As_2)
strong non-fermi liquid behavior (finite intercept)

K-resolved spectral function: hole doping

$Ba_{(1-2x)}K_{2x}Fe_2As_2$

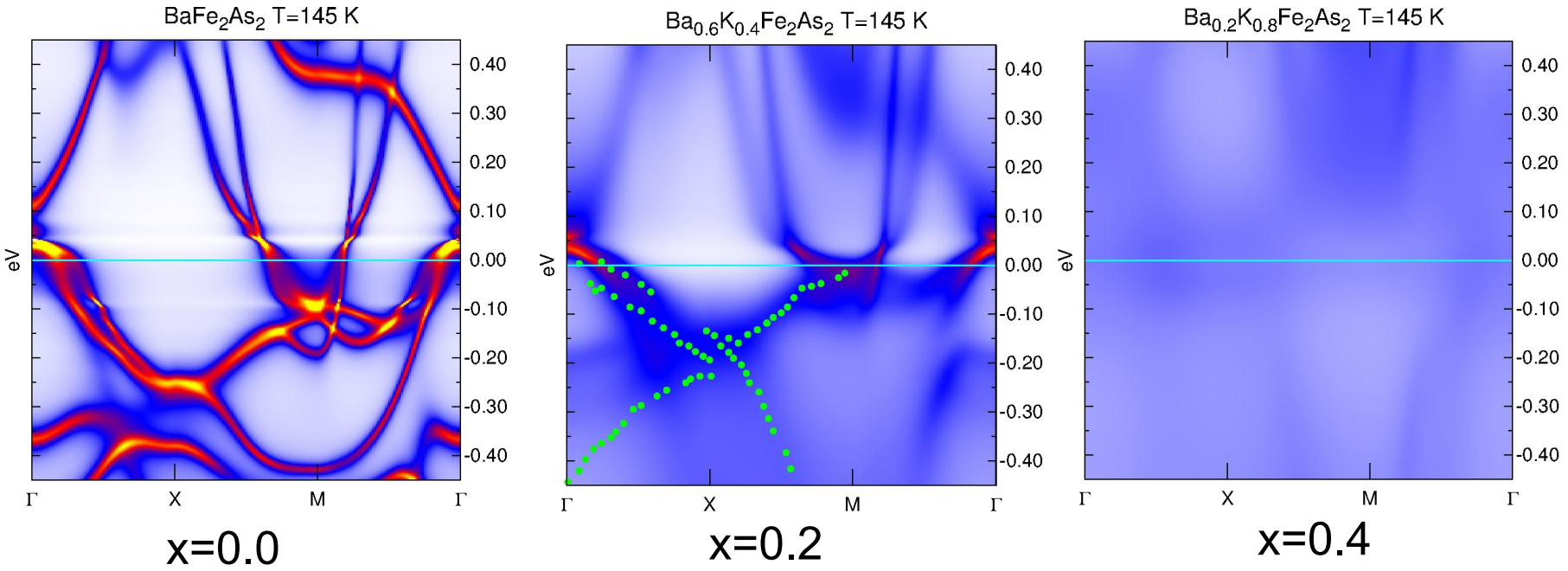

x=0.0 x=0.2 x=0.4

undoped strongly doped

Fermi liquid to non-Fermi liquid crossover

T dependence in the self energy

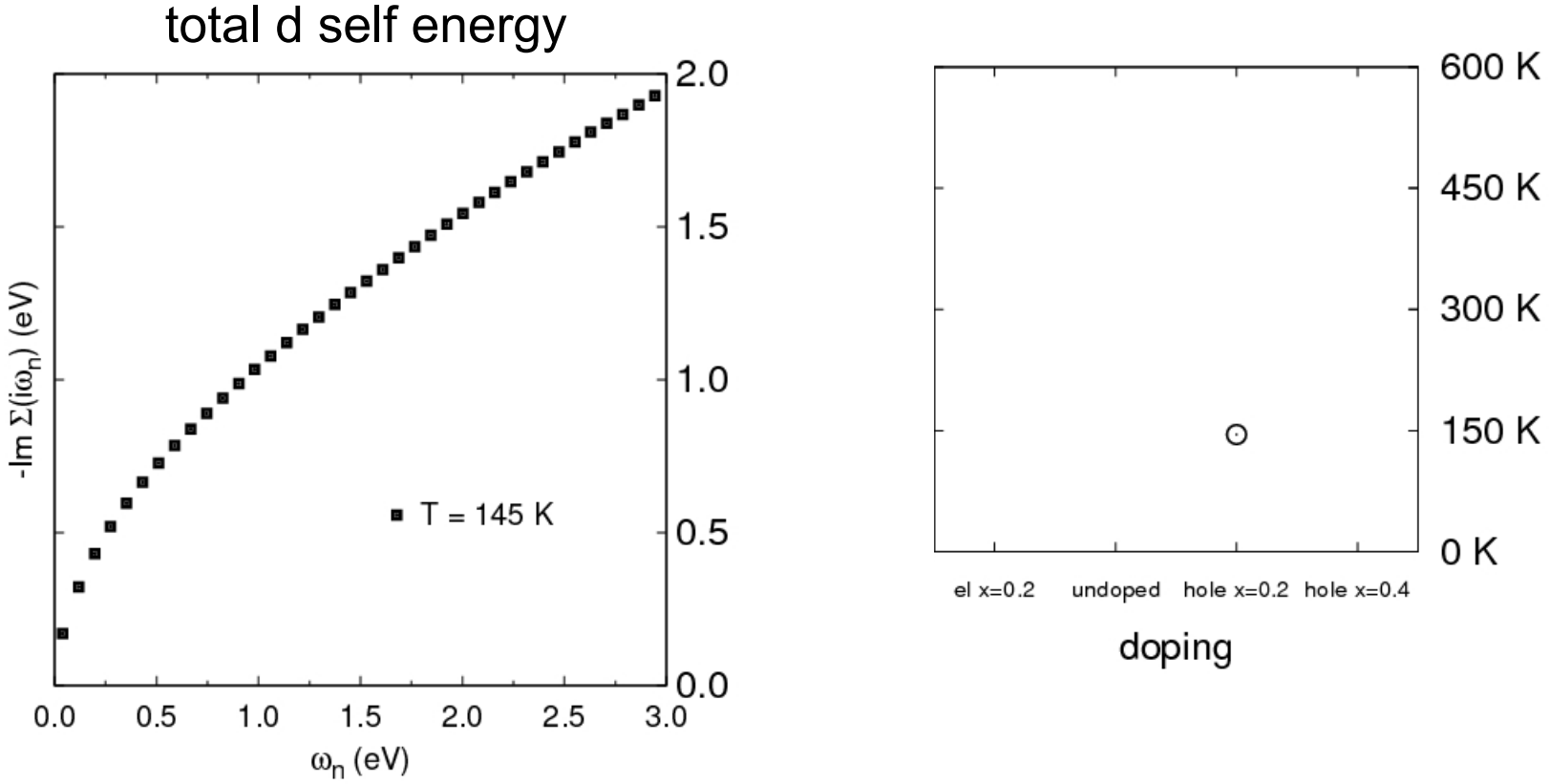

T dependence in the self energy

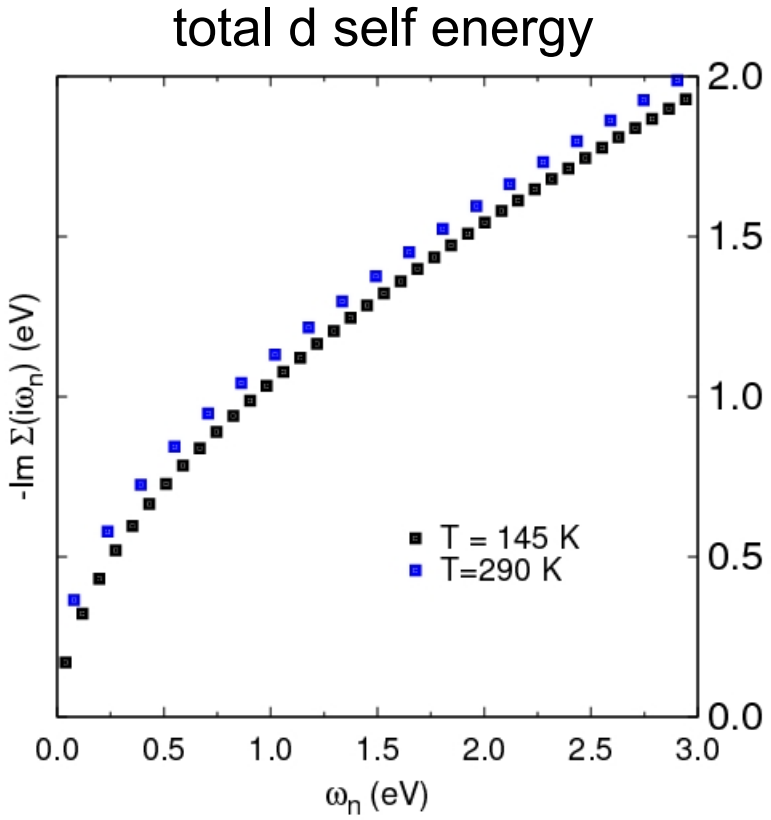

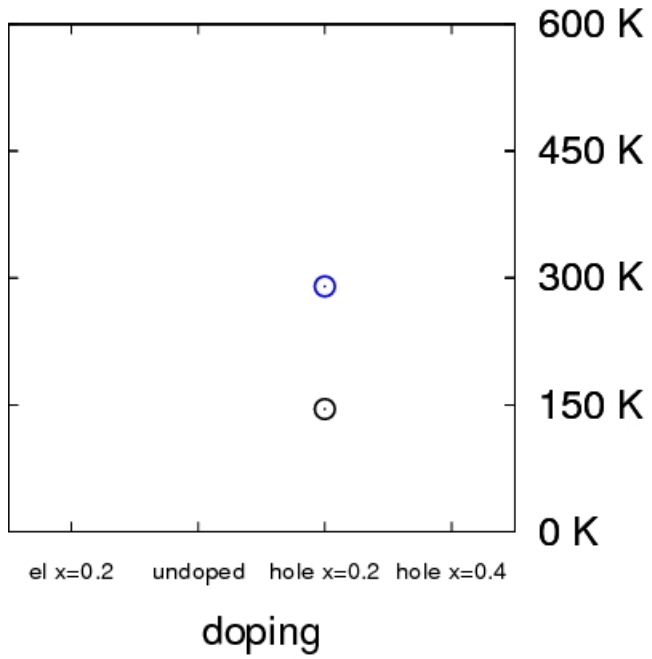

T dependence in the self energy

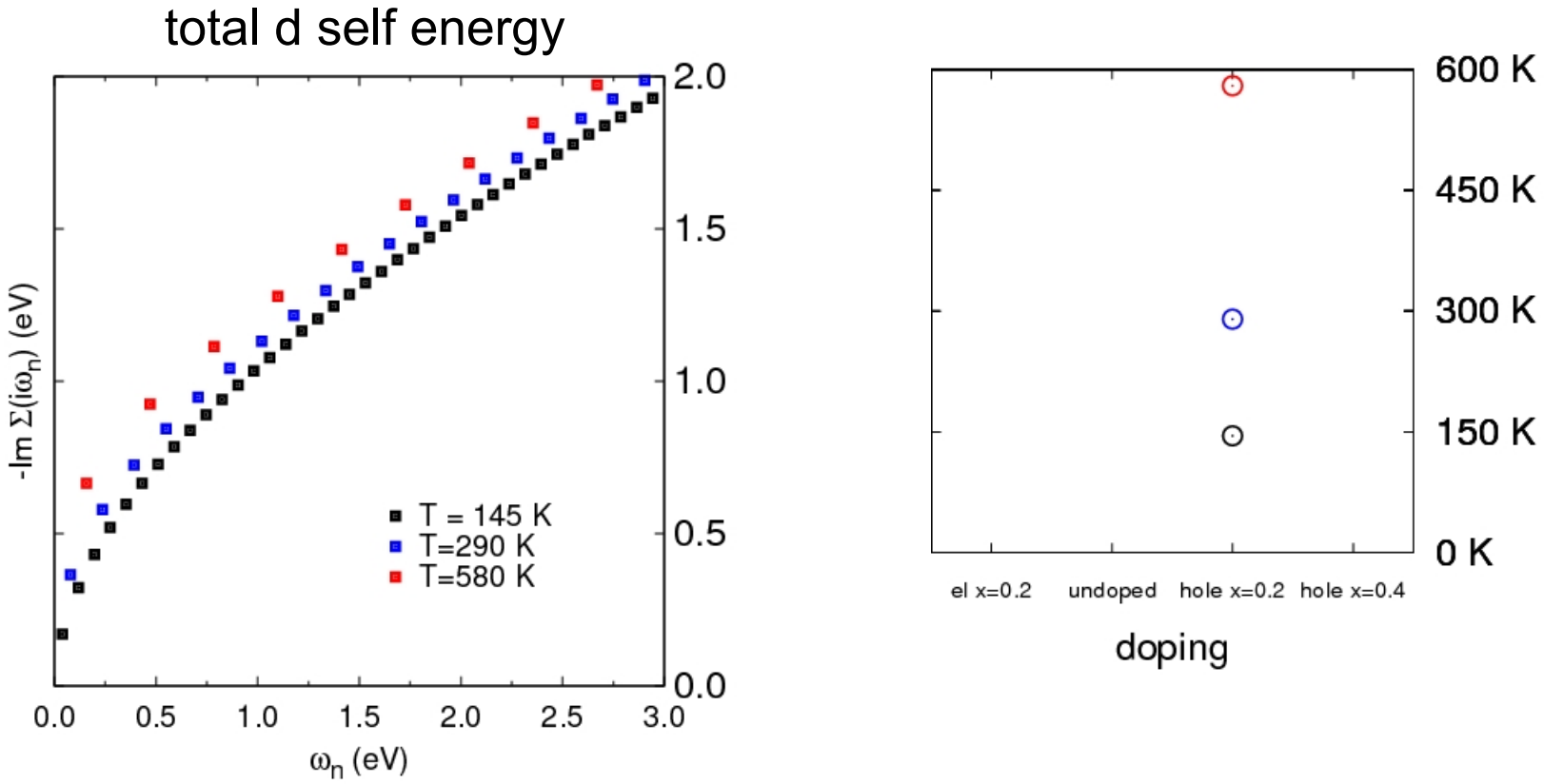

By rising the temperature
the system goes quickly into a strongly incoherent regime

Paramagnetic phase diagram

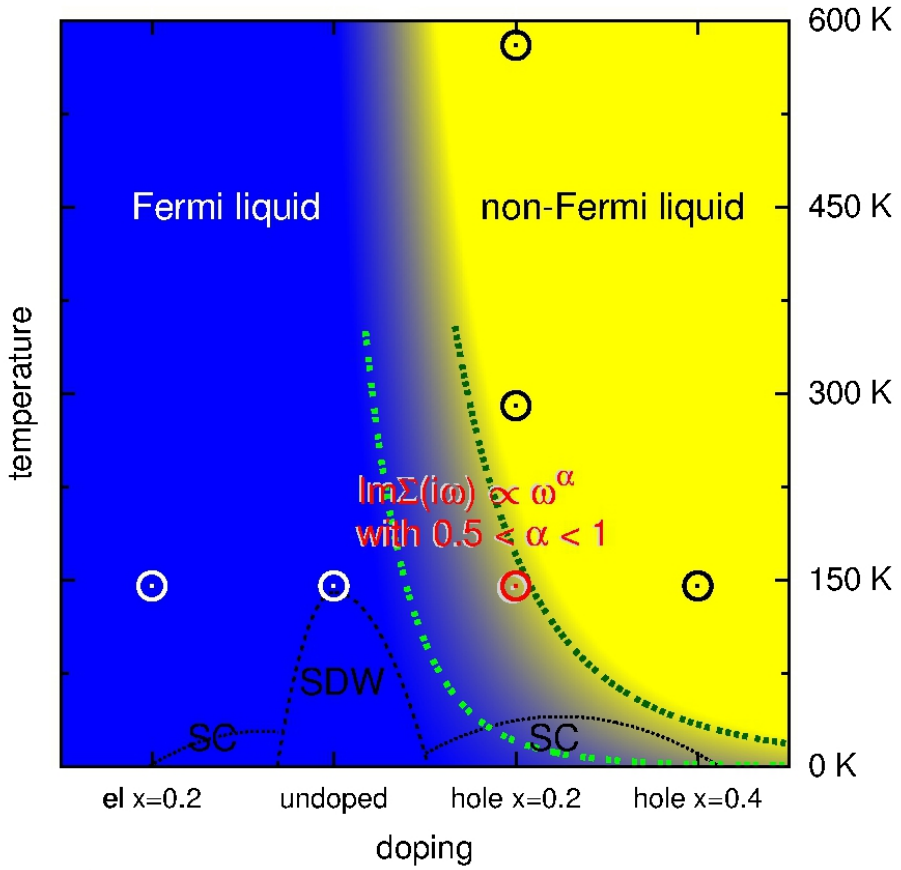

- Electron-hole **asymmetry**
- **Spin-freezing crossover** in the hole doped region

Werner et al. Phys. Rev. Lett. **101**, 166405 (2008), De' Medici et al. PRL **107**, 256401 (2011)

- **Doping dependent renormalization** of the LDA band structure

Comparison to ARPES

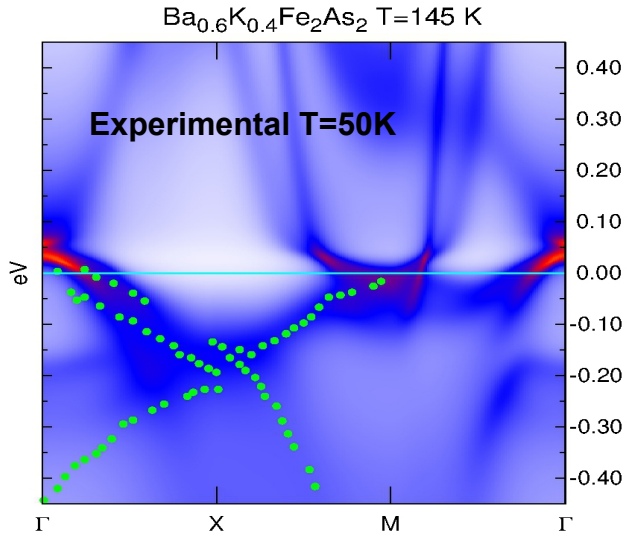

Comparison with Ding et al.
J. Phys.: Cond. Matter **23**, 135701 (2011)

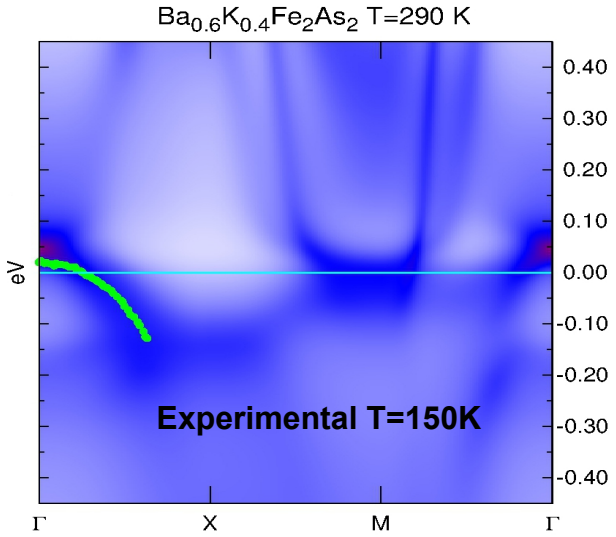

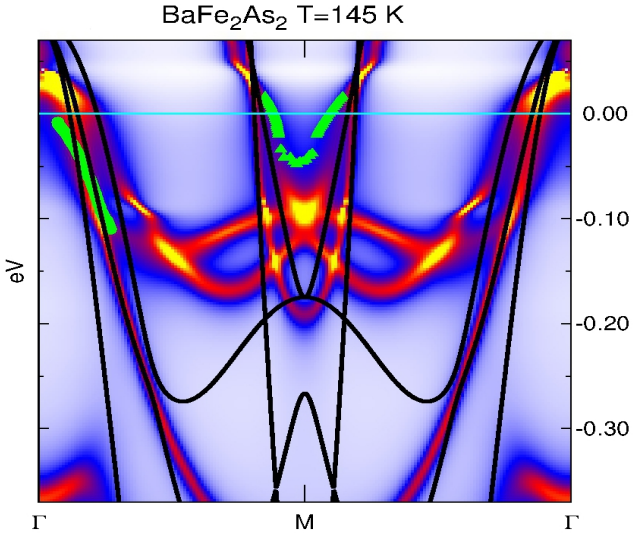

Comparison with V. Brouet et al.
arXiv:1105.5604

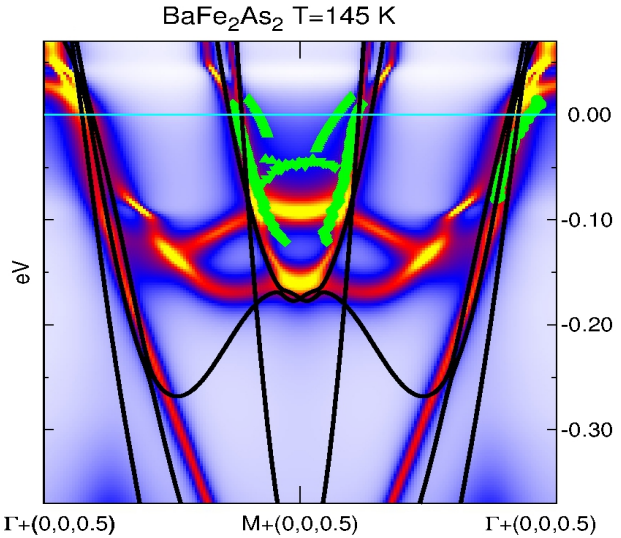

Comparison to ARPES

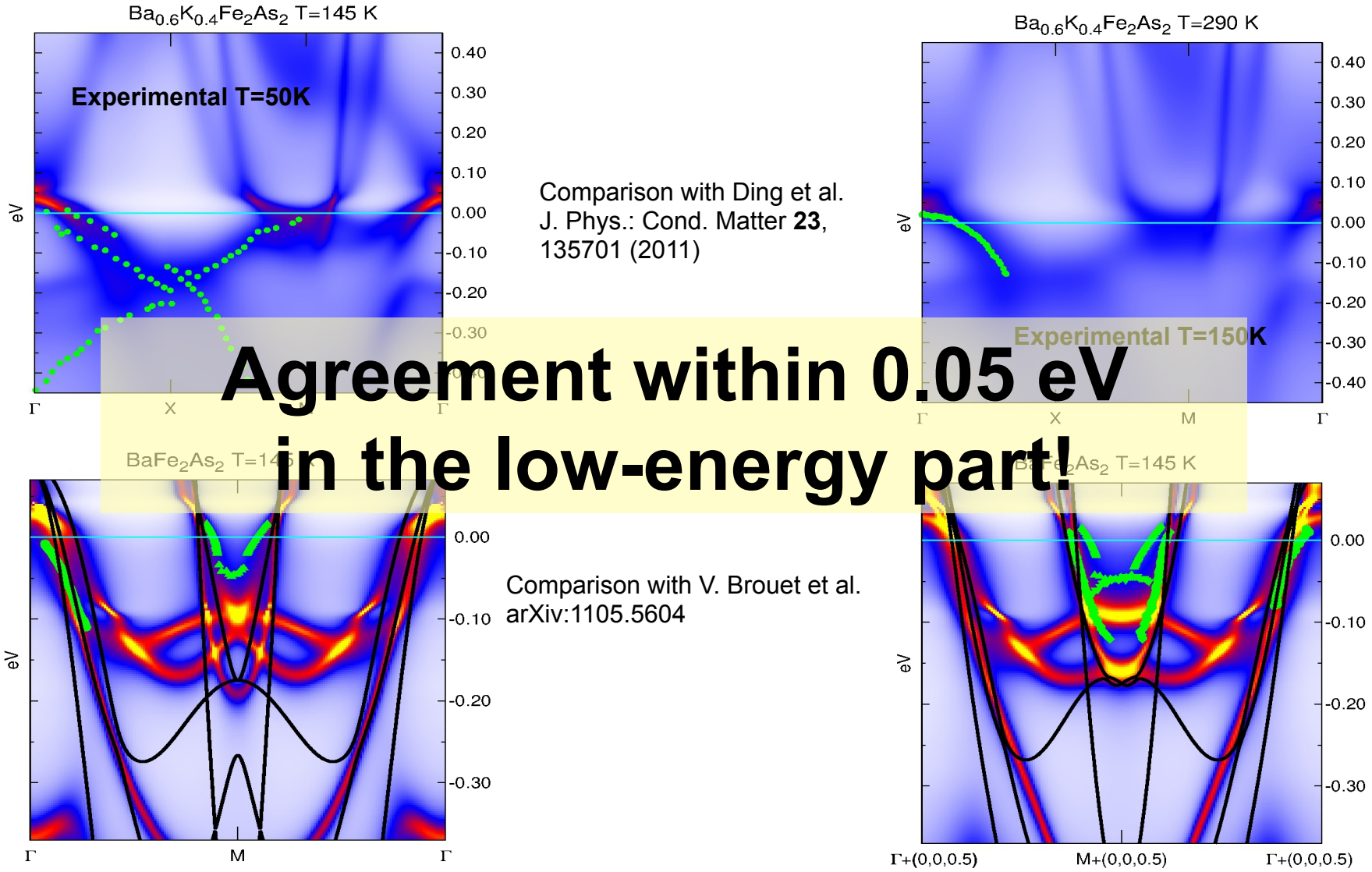

Agreement within 0.05 eV in the low-energy part!

Low-energy effective **static** model

Start from Hubbard-Holstein

$$H = -\sum_{ij\sigma} t_{ij} d^\dagger_{i\sigma} d_{j\sigma} + V \sum_i d^\dagger_{i\uparrow} d_{i\uparrow} d^\dagger_{i\downarrow} d_{i\downarrow} + \mu \sum_{i\sigma} d^\dagger_{i\sigma} d_{i\sigma} + \omega_0 \sum_i b^\dagger_i b_i + \lambda \sum_{i\sigma} d^\dagger_{i\sigma} d_{i\sigma} (b_i + b^\dagger_i).$$

Lang-Firsov transformation

$$H \rightarrow H_{LF} = e^S H e^{-S} \qquad S = \frac{\lambda}{\omega_0} \sum_{i\sigma} n_{i\sigma} (b^+_i - b_i)$$

$$c_{i\sigma} = \exp(\tfrac{\lambda}{\omega_0}(b_i - b^\dagger_i)) d_{i\sigma}$$

$$c^\dagger_{i\sigma} = \exp(\tfrac{\lambda}{\omega_0}(b^\dagger_i - b_i)) d^\dagger_{i\sigma}$$

$$H_{\rm LF} = -\sum_{ij\sigma} t_{ij} c^\dagger_{i\sigma} c_{j\sigma} + U_0 \sum_i c^\dagger_{i\uparrow} c_{i\uparrow} c^\dagger_{i\downarrow} c_{i\downarrow} + \omega_0 \sum_i b^\dagger_i b_i,$$

$$U_0 = V - \frac{2\lambda^2}{\omega_0} \qquad Z_B = \exp(-\lambda^2/\omega_0^2)$$

Projection on the zero-plasmon subspace

$$H_{\rm eff} = \langle 0|H|0\rangle = -\sum_{ij\sigma} Z_B t_{ij} d^\dagger_{i\sigma} d_{j\sigma} + U_0 \sum_i d^\dagger_{i\uparrow} d_{i\uparrow} d^\dagger_{i\downarrow} d_{i\downarrow}$$

Dynamic U effects recovered in the effective static model

Bandwidth renormalization

$$(p^\dagger d^\dagger) \begin{pmatrix} \mathcal{T}_{pp} & \sqrt{Z_B}\mathcal{T}_{pd} \\ \sqrt{Z_B}\mathcal{T}_{pd}^\dagger & Z_B\mathcal{T}_{dd} \end{pmatrix} \begin{pmatrix} p \\ d \end{pmatrix}$$

$$Z_B = \exp\left(1/\pi \int_0^\infty \mathrm{d}\nu \, \mathrm{Im}U_{\mathrm{ret}}(\nu)/\nu^2\right)$$

$$Z_B = 0.59$$

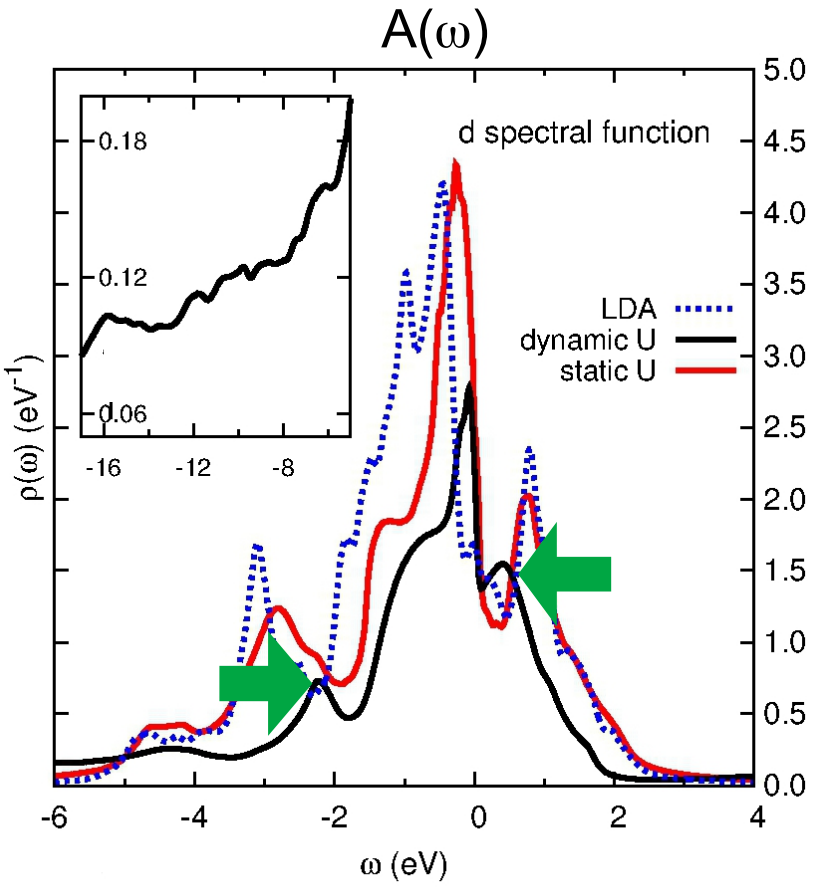

Structures from p-d hybridization squeezed toward the Fermi energy

Dynamic U effects recovered in the effective static model

Green's function renormalization

$$G_{ij}^{\text{low-energy}}(\tau) = -Z_B \langle T d_i(\tau) d_j^\dagger(0) \rangle_{H_{\text{eff}}}$$

loss of spectral weight due to plasmon "shake-up" excitations

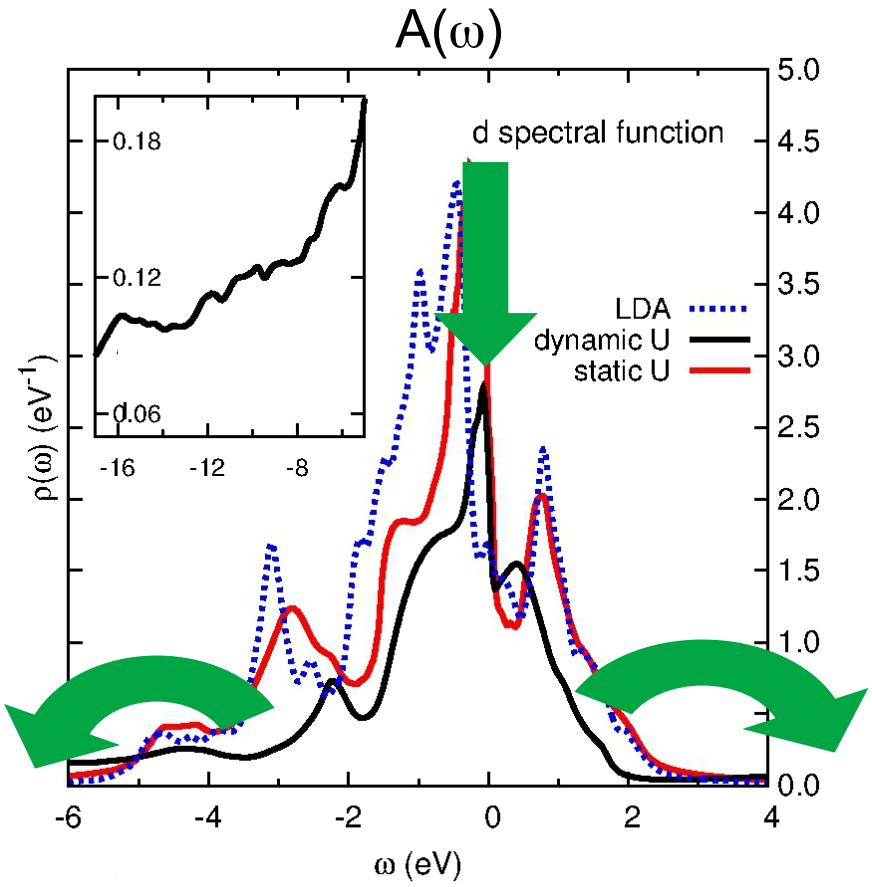

Weight reduction at low-energy and spectral weight transfer to high-energy

cRPA U versus "regular" U

- Static U used in literature for correlated compounds compared to effective U

	Z_B	U_0	U_{lit}
$SrVO_3$	0.70	3.3	4 - 5
Sr_2VO_4	0.70	3.1	4.2
$LaVO_3$	0.57	1.9	5
VO_2	0.67	2.7	4
TaS_2	0.79	1.5	
$SrMnO_3$	0.50	3.1	2.7
$BaFe_2As_2$	0.59	2.8	5
LaOFeAs	0.61	2.7	3.5 - 5
FeSe	0.63	4.2	4 - 5
CuO	0.63	6.8	7.5

The bandwidth renormalization from Coulomb screening explains the apparent contradiction between the static limit of U_{RPA} and the U values used so far in literature

Spectral function in effective low-energy model

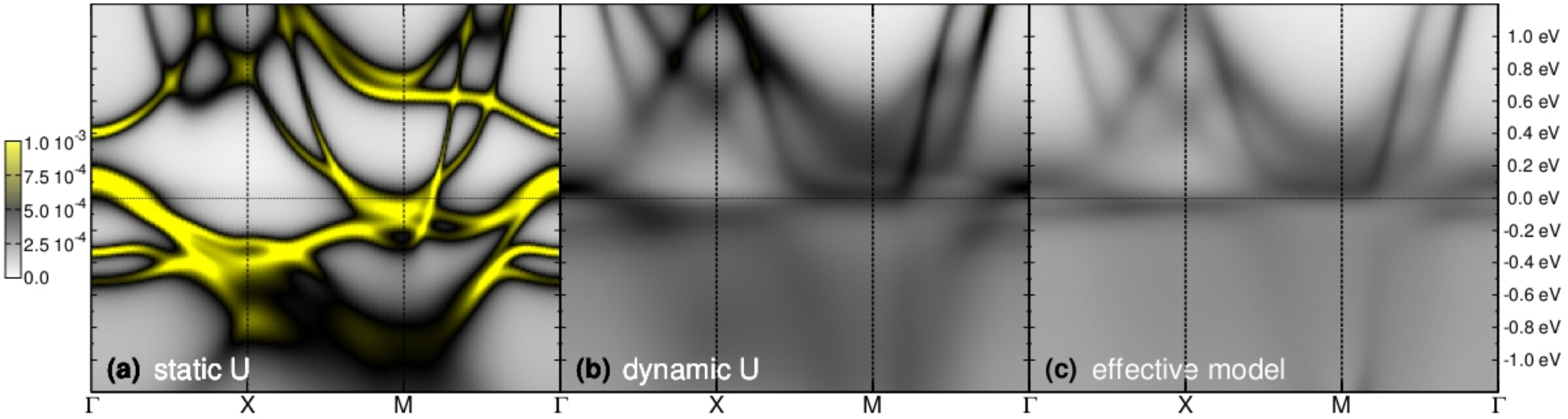

Effective low-energy model spectral function
in agreement with the one obtained for the fully dynamic U model

M. Casula, P. Werner, L. Vaugier, F. Aryasetiawan, A. J. Millis, S. Biermann
PRL **109**, 126408 (2012)

Conclusions

- First ab-initio DMFT calculations with frequency dependent U
- Capability of DMFT to treat plasmon satellites
- Surprises from the strong low-energy impact of the dynamic U, despite the fact that the unscreened part sets on at relatively high energies (~15-20 eV)
- Physical outcome from dynamic part in $BaFe_2As_2$
  - Renormalization of the quasiparticle width and spin-freezing crossover
  - Spectral weight transfer to higher energies
  - Prediction of plasmon satellites
- Effective low-energy model to include dynamic screening

M. Casula, A. Rubtsov, S. Biermann, PRB **85**, 035115 (2012)

P. Werner, M. Casula, T. Miyake, F. Aryasetiawan, A. J. Millis, S. Biermann
Nature Physics **8**, 331-337 (2012)

M. Casula, P. Werner, L. Vaugier, F. Aryasetiawan, A. J. Millis, S. Biermann
PRL **109**, 126408 (2012)